

Master Thesis

The Use of Loaded Antennas as Scattering Relays for Post-Cellular Networks with Closely Spaced Terminals

Autumn Semester 2015

Professor: Armin Wittneben

Supervisor:
Yahia Hassan

Student:
Bernhard Gahr

Declaration of Originality

I hereby declare that the written work I have submitted entitled

Real-Time Demonstrator for ToA based Human Motion tracking System:
Localization and Self-Calibration

is original work which I alone have authored and which is written in my own words.¹

Author(s)

Bernhard Gahr

Student supervisor(s)

Yahia Hassan

Supervising lecturer

Armin Wittneben

With the signature I declare that I have been informed regarding normal academic citation rules and that I have read and understood the information on 'Citation etiquette' (<https://www.ethz.ch/content/dam/ethz/associates/students/studium/exams/files-en/plagiarism-citationetiquette.pdf>). The citation conventions usual to the discipline in question here have been respected.

The above written work may be tested electronically for plagiarism.

Place and date

Signature

¹Co-authored work: The signatures of all authors are required. Each signature attests to the originality of the entire piece of written work in its final form.

Contents

Preface	v
Abstract	vii
Notations, Acronyms and Abbreviations	ix
List of Figures	xi
1 Introduction	1
1.1 Motivation and Goals	1
1.2 State of the Art	2
1.3 Outline	2
2 System	3
2.1 Spatial Channel	4
2.2 Receiver Circuit Description	4
2.2.1 Multiport Networks	4
2.2.2 Receiver Blocks	5
2.2.3 Transfer Function of the Receiver	7
2.2.4 Port Reduction	8
2.2.5 Signal Covariance Matrix	9
2.2.6 Interference Covariance Matrix	9
2.3 Noise Description	9
2.3.1 Antenna Noise	10
2.3.2 LNA Noise	10
2.3.3 Downstream Noise	11
2.3.4 Noise Coupling	11
2.3.5 Noise Covariance Matrix	11
2.4 Rate Calculations	13
3 Analytical Gradient	15
3.1 Signal Gradient	15
3.2 Interference Gradient	16
3.3 Noise Gradients	16
3.3.1 Antenna Noise Gradient	16
3.3.2 LNA Noise Gradient	17
3.3.3 Downstream Noise Gradient	17
3.3.4 Noise Gradient	17

4	Problem Statement and Solver Methods	19
4.1	Utility Function	19
4.1.1	Convexity of the Utility Function	19
4.1.2	Dependency on the Input Power	20
4.1.3	Difference of Local Optima	20
4.1.4	Complexity of the Problem	20
4.2	Gradient Search	21
4.2.1	Choice of Initial Values	21
4.2.2	Adaptive Step Size	22
4.2.3	Conjugate Gradient	22
4.3	Heuristic Optimization Algorithms	24
4.3.1	Simulated Annealing	24
4.3.2	GlobalSearch	24
4.4	Further Algorithm Improvements	26
4.4.1	Optimization of the Interference Function	26
4.4.2	Post Refinement of GlobalSearch by Gradient Search	27
4.4.3	Stepwise Relay Improvements	27
5	Results	31
5.1	Introduction of Measures for Comparison	31
5.1.1	Uncoupled Relay Rates	31
5.1.2	TDMA Rates	32
5.1.3	Signal-Interference-Ration (SIR) Rates	32
5.1.4	Relays as Fully Cooperation Receivers - Limit	32
5.1.5	Multiport Matching - Limit	33
5.2	Relay Placing	33
5.3	Relays to Zeroforce Interference	34
5.3.1	One Interferer	34
5.3.2	Two Interferer	34
5.3.3	Three Interferer	34
5.4	Relay versus Rx Antenna Zeroforcing	34
5.5	Low SNR performance	34
6	Conclusion and Outlook	37
6.1	Conclusion	37
6.2	Future Work	37
	References	39

Preface

I would like to thank Professor Wittneben for giving me the opportunity to work on this semester thesis at the Wireless Communication Group. Further, I want to thank Yahia Hassan, my supervisor, for his help and guidance throughout the thesis.

Abstract

In nowadays wireless networks there are mainly two factors which limit the achievable transmission rates - fading and interference. When multiple-input-multiple-output MIMO systems mostly reduce the impact of fading, the problem of interference has not yet been solved satisfyingly. The most common methods to address the problem of interference are protocols based on schemes like time-division- (TDMA), frequency-division- (FDMA), or code-division multiple access (CDMA). The solution - but in the same time also the downside of those schemes - is the unique allocation of a specific time and/or frequency slot for a single user, hence the blocking of all other users. This effect appears in the pre-logarithmic disproportional factor of the achievable sum rate.

In this thesis we address the problem of interference by the use of passive relay antennas (short: passive relays), i.e. antennas with only passive, lossless impedances attached, which interact with the receiving antennas only by the effect of coupling. By the choice of the passive elements the effect of the coupling can be changed and by using multiple passive relays, the coupling can be used to increase the signal- and reduce the interference power at the receivers.

In the following, a new description of the system will be derived, which allows an easier, more elegant way of analyzing the effect of coupling. Different solver methods are analyzed and discussed in order to find an optimal choice of the relay impedances. As some of the solvers are based on the method of gradient search, the analytical gradient will be derived. For the gradient search method, a variety of initial value choices will be compared to each other. Further, the results are evaluated and compared to previously known methods.

Notations, Acronyms and Abbreviations

Symbols

\mathbf{x}	Vector
$\mathbf{x}[i]$ or \mathbf{x}_i	i-th element of vector \mathbf{x}
$\ \mathbf{x}\ $	2-norm of vector \mathbf{x}
$\ \mathbf{x}\ _p$	LP-norm of vector \mathbf{x}
\mathbf{X}	Matrix
\mathbf{X}^T	transpose of matrix \mathbf{X}
\mathbf{X}^{-1}	inverse of matrix \mathbf{X}

Indices

x, y, z	x, y, z axis
-----------	--------------

Acronyms and Abbreviations

ETH	Eidgenössische Technische Hochschule
WCG	Wireless Communicatoin Group
UWB	Ultra-Wide Band
HMT	Human Motion Tracking
CIR	Channel Impulse Response
(N)LOS	(Non) Line of Sight
DSSS	Direct-Sequence Spread Spectrum
(A,T,TD)oA	(Angle,Time,Time Difference) of Arrival
ML	Maximum Likelihood
SDP	Semidefinite Programming
CDF	Cummulative Distribution Function
PDF	Probability Density Function
RMSE	Root Mean Squared Error

List of Figures

2.1	Overview of the system.	3
2.2	Example of the receive antenna and the relay placing.	4
2.3	A twoport network [2].	5
2.4	The receiver, with the coupling network \mathbf{Z}_C , the SP-matching network \mathbf{Z}_M , the LNA, and loads attached to the LNA.	6
2.5	Port reduction on a network with one load connected to the last port.	8
2.6	An example of the matrix shaping function. On the left the matrix shaped by $\Gamma(\cdot)$ on the right the matrix shaped by $\Gamma(\cdot)^{-1}$. The sub matrices \mathbf{A} , \mathbf{B} and \mathbf{C} are square matrices and lie on the diagonal.	12
4.1	The utility function for different imaginary relay impedances for two relays and two different channel realizations.	20
4.2	The sum rate over the gradient search iterations.	21
4.3	Comparison of the number of initial values used.	21
4.4	Schematic of the adaptive step size algorithm.	22
4.5	A comparison of the convergence of gradient descent with optimal step size (in green) and conjugate vector (in red) for minimizing a quadratic function associated with a given linear system[8].	22
4.6	Comparison between Steepest Ascent, Polak-Ribière, and Fletcher-Reeves.	23
4.7	Comparison of the Simulated Annealing algorithm for different number of initializations and the results from "Polak-Ribière" and "Steepest Ascent" gradient searches.	24
4.8	Schematics of the GlobalSearch and MultiStart algorithms [13].	25
4.9	Performance of the GlobalSearch algorithm in comparison to the previous results.	25
4.10	Comparison of the number of initial values used.	26
4.11	Comparison the heuristic solvers with and without a post refinement by gradient search.	27
4.12	Comparison of the number of initial values used.	28
4.13	Example of choosing the relays for stepwise optimization.	28
5.1	Comparison of uncoupled relays and optimized coupled relays.	31
5.2	Comparison of the TDMA rate and optimized coupled relays.	32
5.3	Comparison of the full cooperation relay rates, the multiport matching rate and optimized coupled relays rate.	33
5.4	Placing the relays around a receiver uniformly distributed on a disk.	34
5.5	Sum rates for one interferer and one receiver with $N_{\text{Rel}} \in \{1, 2, 3\}$	35
5.6	Sum rates for two interferer and one receiver with $N_{\text{Rel}} \in \{2, 3, 4, 5\}$	35
5.7	Sum rates for three interferer and one receiver with $N_{\text{Rel}} \in \{4, 5, 6, 7\}$	35

Chapter 1

Introduction

Future wireless networks are assumed to be of higher density at the receiver side, as more and more devices with access to the internet are appearing on the market, and more and more types of devices are staffed with modules which are able to connect to the internet (internet of things IoT). Examples for such scenarios are cellular networks in an urban area, wireless networks in public spaces as concert halls, or sensor networks.

Such networks mainly suffer from two rate limiting effects: fading and interference. When the effect of fading is mostly solved by MIMO-techniques, the interference is the remaining bottleneck to achieve high data rates. Current methods to overcome interference are protocols like TDMA, FDMA or CDMA. The downside of those protocols is the unique allocation of a user to a specific time or frequency slot, hence the blocking of all other users for this period. More advanced techniques use multiple antennas as in the case of fading, to achieve multiple observations of the incoming signals and therefore the ability to zero-force the interfering signals. This, however, is only possible, if the number of antennas per receiver is larger than the number of interfering signal streams ?? - in high density networks nearly impossible, or very expensive as the size of the receiver structure grows rapidly.

In this thesis the use of passive relays, i.e. antennae with pure imaginary impedances attached is introduced. As they are placed very closely (in terms of wavelengths) around the receivers, they interact by the effect of coupling with the receivers. By the choice of the impedances, the strength of coupling can be changed. With an increasing number of such passive relays, the coupling can be used to steer the signal towards the receiver and block the interference.

1.1 Motivation and Goals

The achievable rate of a connection pair is proportional to the signal to noise and interference ratio (SINR) (??). In a high power region the effect of noise can be neglected as the interference is the main diminishing factor. Therefore an interference-free connection is the main goal.

As the method of using passive relays only by their coupling is a new way of addressing the problem of interference, this thesis will look more into the achievable improvements than into the feasibility of the method. To achieve the highest possible rate for any realization, the shape of the problem will be analyzed and different solver methods will be introduced and compared.

1.2 State of the Art

TBD...

Nossekk Ivrlac Hassan Wittneben

1.3 Outline

In the following chapter the whole system will be described. The effect of coupling will be analyzed and the overall transfer function - from the transmitter to the receiver will be stated. All the noise sources appearing in the systems and their transfer function will be shown and derived. The transfer functions will be splitted up into smaller, simpler (sub-) functions, so that the effect of coupling and the interference can be better described and analyzed.

As one of the solver methods is gradient search, in the third chapter the analytical gradients will be derived - for the signal, the interference and the noise part. The gradient is dependent on the covariance matrix, therefore they will be derived as well for the signal, interference and noise contributions at the receiver.

Last, the different solver methods will be evaluated. The results will be compared versus the number of relays used in a setup, versus different types of placings of the relays and versus different numbers of connection pairs. Additionally theoretical limits of the setups will be derived and the results will be compared to current protocols which overcome interference (TDMA).

Chapter 2

System

In the following the system will be described. Figure 2.1 gives an overview of it. The transmitters on the left are assumed to be widely spaced, so that they experience no coupling among each other. The signals are transmitted over a spatial interference channel, therefore a transmitted signal reaches every receiver.

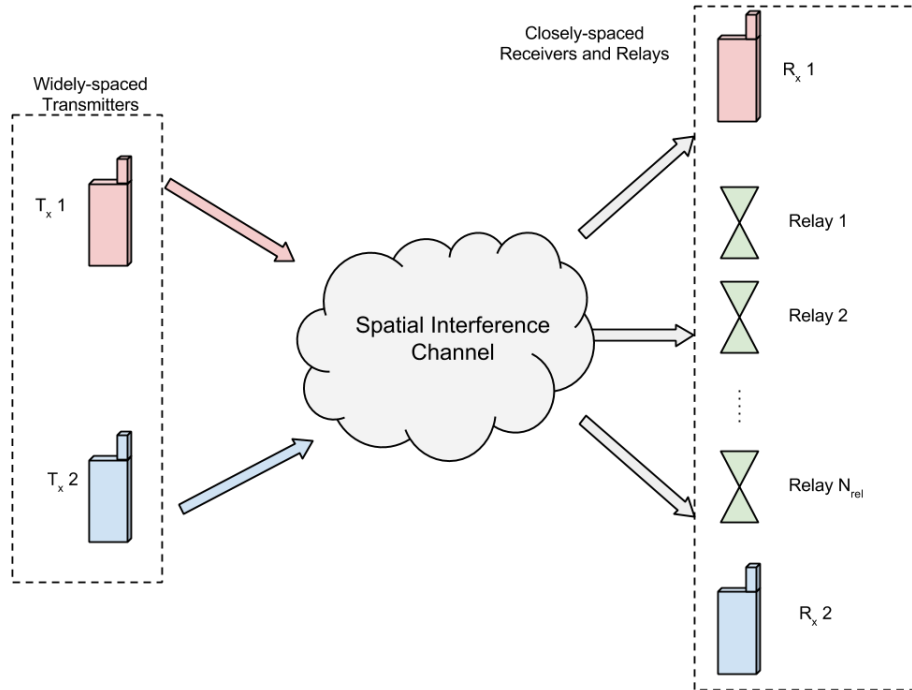


Figure 2.1: Overview of the system.

Besides the receivers, there are passive relays on the right side. The relays and the receivers are closely spaced, therefore the channels between a transmitter and the receivers and relays are spatially correlated and the elements on the receiver side experience coupling among each other.

2.1 Spatial Channel

As mentioned in the previous section the spatial channel is generated by spatial correlation among the receivers and the relays, dependent on the distance. The correlation matrix is generated by the besselfuntion according to

$$\mathbf{R}_{i,j} = B(2 \cdot d_{i,j} \cdot \pi, 0), \quad (2.1)$$

where $B(d, 0)$ is the 0-th bessel function and $d_{i,j}$ the distance between the i -th and j -th receiving element (receive antennas and relays concatenated). Therefore \mathbf{R} is symmetric and 1 on its diagonal, as $B(0, 0) = 1$.

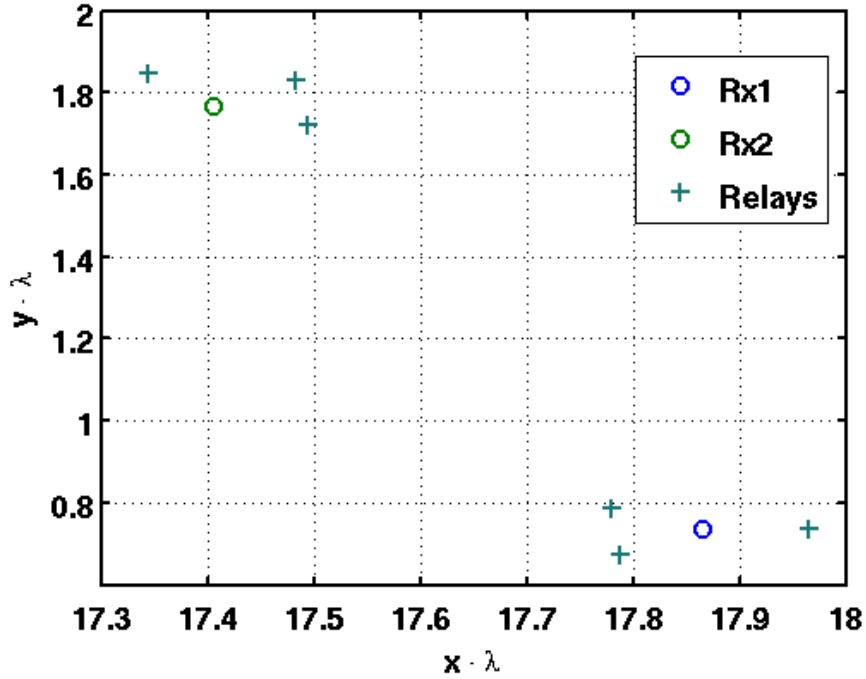


Figure 2.2: Example of the receive antenna and the relay placing.

The spatial channel from j -th transmitter to all receivers and relays is then generated by

$$\mathbf{H}_j^{\text{sp}} = \mathbf{R}^{\frac{1}{2}} \cdot \mathbf{\Delta}, \quad (2.2)$$

where $\mathbf{\Delta}$ is a matrix with complex elements drawn from the standard normal distribution ($\mu = 0$ and $\sigma = 1$). Therefore \mathbf{H}_j^{sp} is of size $N_{\text{User}} \cdot (N_{\text{Rx}} + N_{\text{Rel}}) \times N_{\text{Tx}}$.

2.2 Receiver Circuit Description

As mentioned in Section 1.2, the idea of describing the receiver circuitry is based on the work of [1]. To do so, we represent each receiver block (shown in Figure 2.4) by n-ports. A short overview on 2-ports (simplified n-ports) is given in the following.

2.2.1 Multiport Networks

In the following a 2-port network will be analyzed. Later this can be easily extended to a multiport network.

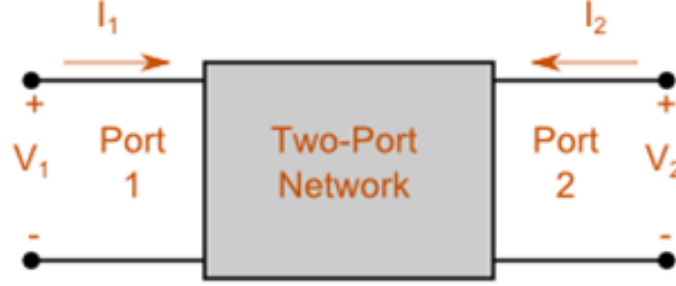


Figure 2.3: A twoport network [2].

Figure 2.3 shows a 2-port network. The twoport network can be represented by an impedance matrix \mathbf{Z} . The elements Z_{ij} of the matrix are defined in the following way:

$$Z_{ij} = \frac{V_i}{I_j}, \quad (2.3)$$

for the currents $I_l = 0, \quad l \neq j$.

Therefore the 2-port's input/output relations can be written as

$$\begin{bmatrix} V_1 \\ V_2 \end{bmatrix} = \mathbf{Z} \cdot \begin{bmatrix} I_1 \\ I_2 \end{bmatrix} \quad (2.4)$$

For a multiport network, elements V_1, V_2, I_1 and I_2 become vectors, and the elements Z_{ij} , $i, j \in \{1, 2\}$ become submatrices. Looking from the left into the network with a load R_L attached to port two, the equivalent input impedance becomes

$$\mathbf{Z}_{in_1} = \mathbf{Z}_{11} - \mathbf{Z}_{21} \cdot (\mathbf{Z}_{22} + R_L \cdot \mathbf{I})^{-1} \cdot \mathbf{Z}_{12}. \quad (2.5)$$

With no load attached on port two, the equivalent input impedance becomes

$$\mathbf{Z}_{in_1} = \mathbf{Z}_{11}. \quad (2.6)$$

Last, having port one short-circuited and looking from port two into the network, the equivalent network impedance becomes

$$\mathbf{Z}_{in_2} = \mathbf{Z}_{22} - \mathbf{Z}_{12} \cdot (\mathbf{Z}_{11})^{-1} \cdot \mathbf{Z}_{21}. \quad (2.7)$$

For reciprocal (multiport-)networks (RLC -Networks, containing only passive elements), $\mathbf{Z}_{12} = \mathbf{Z}_{21}^T$.

2.2.2 Receiver Blocks

The receiver (as shown in Figure 2.4) consists of three blocks. From left to right:

1. the coupling network (\mathbf{Z}_C),
2. the matching network (\mathbf{Z}_M), and
3. the low-noise-amplifier (**LNA**).

All these blocks can be described in multiport networks. In the following each block will be discussed.

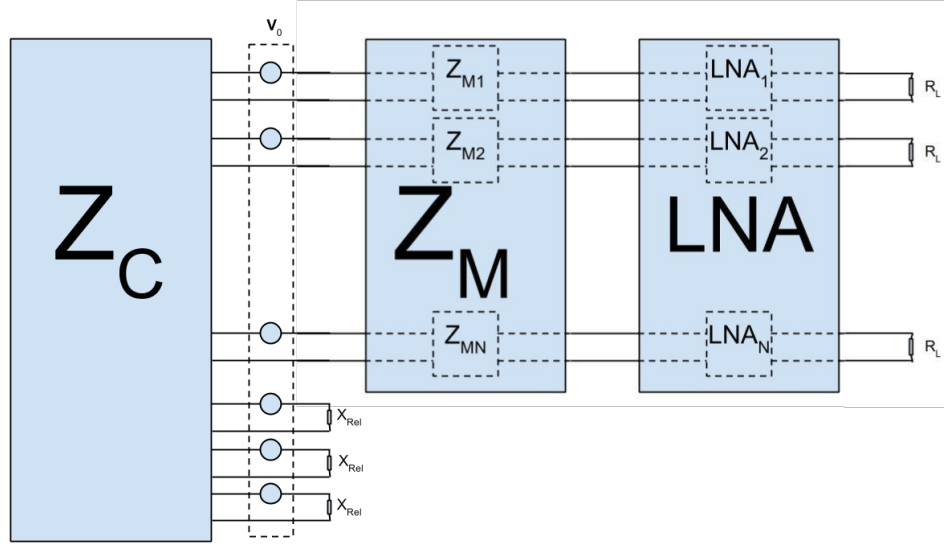


Figure 2.4: The receiver, with the coupling network \mathbf{Z}_C , the SP-matching network \mathbf{Z}_M , the LNA, and loads attached to the LNA.

The Coupling Network

The coupling network comes from the fact, that compact antenna arrays are used. The strength of the coupling between two antennas depends on the spacing between the antennas. In the following a uniform spacing of the antennas is assumed. As the effect of coupling from one antenna to another is the same like the reverse, the impedance matrix \mathbf{Z}_C becomes symmetric.

The Matching Network

Behind the each receiving antenna a matching network placed, to improve the performance of the receiver. For complexity and bandwidth reasons ("WCNC - Paper"), single-port (SP) matching is assumed. The matching network has the form of

$$\mathbf{Z}_M = \begin{bmatrix} \mathbf{Z}_{M11} & \mathbf{Z}_{M12} \\ \mathbf{Z}_{M21} & \mathbf{Z}_{M22} \end{bmatrix}. \quad (2.8)$$

For a matching network to be lossless it must be pure imaginary and symmetric[1]. Because we assume SP matching the submatrices become diagonal, with the additional property of $\mathbf{Z}_{M12} = \mathbf{Z}_{M21}^T \implies \mathbf{Z}_{M12} = \mathbf{Z}_{M21}$.

The Low-Noise-Amplifier

In the LNA-block the received signal after the matching network gets amplified. As in the matching network the LNA can be represented in the following way

$$\mathbf{LNA} = \begin{bmatrix} \mathbf{c} & \mathbf{d} \\ \mathbf{e} & \mathbf{g} \end{bmatrix}. \quad (2.9)$$

As each branch has its own LNA, the submatrices \mathbf{c} , \mathbf{e} and \mathbf{g} are again diagonal. Additionally, matrix \mathbf{d} is an all-zeros matrix if the unilateral assumption (*the input of the LNA is not affected by the output of the LNA*) is applied.

2.2.3 Transfer Function of the Receiver

The main interest lies in the transfer function of the input voltages \mathbf{v}_0 to the voltage measured at the loads (in Figure 2.4) \mathbf{v}_L . In the following the transferfunction over each block of the receiver will be derived. We use the termination: \mathbf{v}_i is the voltage on the left of the block i (i.e. v_M is the voltage on the left ports of the matching network). Additionally, we see the left ports as input ports and the right ports as output ports of each block.

For the derivation of the transferfunction we need four equivalent impedance matrices, namely

1. \mathbf{Z}_{eqM_1} , the impedance matrix looking from the left into the matching network,
2. \mathbf{Z}_{eqM_2} , the impedance matrix looking from the right into the matching network,
3. \mathbf{Z}_{eqLNA_1} , the impedance matrix looking from the left into the LNA, and
4. \mathbf{Z}_{eqLNA_2} , the impedance matrix looking from the right into the LNA.

To calculate \mathbf{Z}_{eqM_1} and \mathbf{Z}_{eqLNA_1} , we use Equation (2.5) and get the following

$$\mathbf{Z}_{eqM_1} = \mathbf{Z}_{M11} - \mathbf{Z}_{M21} \cdot (\mathbf{Z}_{M22} + \mathbf{Z}_{eqLNA_1})^{-1} \cdot \mathbf{Z}_{M12}, \quad (2.10)$$

$$\mathbf{Z}_{eqLNA_1} = \mathbf{c} - \mathbf{e} \cdot (R_L \mathbf{I}_{N_r} + \mathbf{g})^{-1} \cdot \mathbf{d} = \mathbf{c}. \quad (2.11)$$

As we step through the receiver blocks from left to right, we always have the parallel voltages applied to each receiver block on the left. Therefore the equivalent input impedances \mathbf{Z}_{eqM_2} and \mathbf{Z}_{eqLNA_2} can be derived using Equation (2.6) and lead to the following

$$\mathbf{Z}_{eqM_2} = \mathbf{Z}_{M22} - \mathbf{Z}_{M12} \cdot (\mathbf{Z}_{M11})^{-1} \cdot \mathbf{Z}_{M21}, \quad (2.12)$$

$$\mathbf{Z}_{eqLNA_2} = \mathbf{g} - \mathbf{d} \cdot (\mathbf{c})^{-1} \cdot \mathbf{e} = \mathbf{g}. \quad (2.13)$$

To get the parallel input voltage on the left of the matching network, we use the principle of a voltage divider as

$$\mathbf{v}_M = \mathbf{Z}_{eqM_1} \cdot (\mathbf{Z}_{eqM_1} + \mathbf{Z}_C)^{-1} \cdot \mathbf{v}_0 \quad (2.14)$$

To transfer the voltages from the left ports to the right ports of each block we proceed for each block in the following:

1. Calculate the input currents,
2. transfer the input currents to the output voltages in series, and
3. calculate the output voltages in parallel, by a voltage divider.

For the matching network, it follows:

$$\mathbf{i}_M = \mathbf{Z}_{M11}^{-1} \cdot \mathbf{v}_M, \quad (2.15)$$

$$\mathbf{v}_{LNA_{series}} = \mathbf{Z}_{M12} \cdot \mathbf{i}_M = \mathbf{Z}_{M12} \mathbf{Z}_{M11}^{-1} \cdot \mathbf{v}_M, \quad (2.16)$$

$$\begin{aligned} \mathbf{v}_{LNA} &= \mathbf{Z}_{eqLNA_1} (\mathbf{Z}_{eqLNA_1} + \mathbf{Z}_{eqM_2})^{-1} \cdot \mathbf{v}_{LNA_{series}} \\ &= \mathbf{Z}_{eqLNA_1} (\mathbf{Z}_{eqLNA_1} + \mathbf{Z}_{eqM_2})^{-1} \mathbf{Z}_{M12} \mathbf{Z}_{M11}^{-1} \cdot \mathbf{v}_M, \end{aligned} \quad (2.17)$$

and equivalent for the LNA block

$$\mathbf{v}_L = R_L \mathbf{I}_{N_r} (R_L \mathbf{I}_{N_r} + \mathbf{Z}_{LNA_2})^{-1} \mathbf{Z}_{LNA_{12}} \mathbf{Z}_{LNA_{11}}^{-1} \cdot \mathbf{v}_{LNA}. \quad (2.18)$$

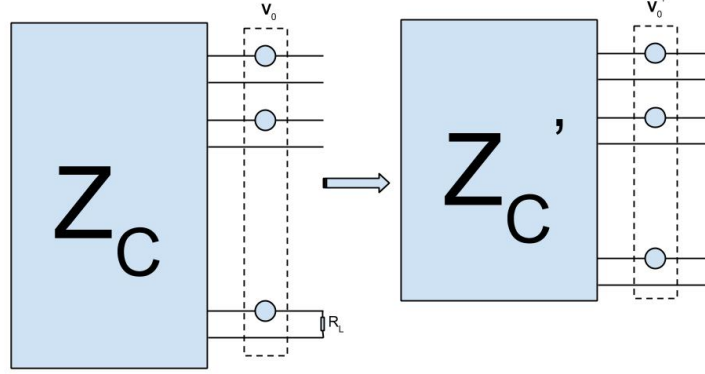


Figure 2.5: Port reduction on a network with one load connected to the last port.

Therefore we have three transfer functions to characterize our system. Denoting the transfer function from voltage \mathbf{v}_j to voltage \mathbf{v}_i as $\mathbf{H}_{i,j}$ (i.e. $\mathbf{v}_i = \mathbf{H}_{i,j} \cdot \mathbf{v}_j$), it follows

$$\mathbf{H}_{M,0'} = \mathbf{Z}_{eqM_1} \cdot (\mathbf{Z}_{eqM_1} + \mathbf{Z}_C)^{-1}, \quad (2.19)$$

$$\mathbf{H}_{LNA,M} = \mathbf{Z}_{eqLNA_1} (\mathbf{Z}_{eqLNA_1} + \mathbf{Z}_{eqM_2})^{-1} \mathbf{Z}_{M12} \mathbf{Z}_{M11}^{-1}, \quad \text{and} \quad (2.20)$$

$$\mathbf{H}_{L,LNA} = R_L \mathbf{I}_{N_R} (R_L \mathbf{I}_{N_R} + \mathbf{Z}_{eqLNA_2})^{-1} \mathbf{Z}_{LNA12} \mathbf{Z}_{LNA11}^{-1}. \quad (2.21)$$

And the overall transferfunction

$$\mathbf{H}_{L,0'} = \mathbf{H}_{L,LNA} \cdot \mathbf{H}_{LNA,M} \cdot \mathbf{H}_{M,0'}. \quad (2.22)$$

2.2.4 Port Reduction

In the following we describe the open circuit reduction of a system like in Figure 2.5. We do the port reduction, because we are interested in the signal only at the loads of some receivers. The signal picked up at relay antennae or not considered receivers contributes to the considered receiver by the coupling between the antennae, as described in Section 2.2.2. Passive antennas (e.g. relay antennas) can be modeled by connecting a load directly onto the coupling network as shown in Figure 2.5. Undesired receivers can be equivalently modelled, however in this case, the load corresponds to the equivalent input impedance, when looking from the left into the matching network (as in Equation (2.10)). In the following, \mathbf{v}_C denotes the voltages on the ports between the coupling matrix \mathbf{Z}_C and the voltage sources \mathbf{v}_0 , the same for the currents. As we are not interested in the input/output-relation of these passive antennas, a port reduction is performed. For the port reduction, the coupling matrix \mathbf{Z}_C can be represented by four submatrices

$$\mathbf{Z}_C = \begin{bmatrix} \mathbf{Z}_{OO} & \mathbf{Z}_{OL} \\ \mathbf{Z}_{LO} & \mathbf{Z}_{LL} \end{bmatrix}, \quad (2.23)$$

so that we get the system relations

$$\begin{bmatrix} \mathbf{v}_{CO} \\ \mathbf{v}_{CL} \end{bmatrix} = \begin{bmatrix} \mathbf{Z}_{OO} & \mathbf{Z}_{OL} \\ \mathbf{Z}_{LO} & \mathbf{Z}_{LL} \end{bmatrix} \cdot \begin{bmatrix} \mathbf{i}_{CO} \\ \mathbf{i}_{CL} \end{bmatrix}. \quad (2.24)$$

The index "O" denotes hereby the open circuit ports, the index "L" the ports with a load attached. We assume, that there are N_R antennas, whereby the first N_i

antennas are active, and the later ones are passive (and therefore modeled by a load). \mathbf{Z}_{pass} denotes in the following the $N_r - N_i$ loads representing the passive antennas. Therefore it is a diagonal matrix.

From Equation (2.24) and the property

$$\mathbf{v}_{CL} = \mathbf{v}_0[N_i + 1 : N_R] - \mathbf{Z}_{pass} \cdot \mathbf{i}_{CL} \quad \text{it follows,} \quad (2.25)$$

$$\begin{aligned} \mathbf{i}_{CL} = & -(\mathbf{Z}_{pass} + \mathbf{Z}_{LL})^{-1} \mathbf{Z}_{LO} \cdot \mathbf{i}_{CO} - \\ & (\mathbf{Z}_{pass} + \mathbf{Z}_{LL})^{-1} \cdot \mathbf{v}_0[N_i + 1 : N_R] \end{aligned} \quad (2.26)$$

and therefore,

$$\begin{aligned} \mathbf{v}_{CO} = & (\mathbf{Z}_{OO} - \mathbf{Z}_{OL}(\mathbf{Z}_{pass} + \mathbf{Z}_{LL})^{-1} \mathbf{Z}_{LO}) \cdot \mathbf{i}_{CO} - \\ & \mathbf{Z}_{OL}(\mathbf{Z}_{pass} + \mathbf{Z}_{LL})^{-1} \cdot \mathbf{v}_0[N_i + 1 : N_R]. \end{aligned} \quad (2.27)$$

With this port reduction we have the new coupling matrix and the new voltage input as

$$\mathbf{Z}'_C = \mathbf{Z}_{OO} - \mathbf{Z}_{OL}(\mathbf{Z}_{pass} + \mathbf{Z}_{LL})^{-1} \mathbf{Z}_{LO} \quad \text{and} \quad (2.28)$$

$$\mathbf{v}'_0 = \mathbf{H}_0 \cdot \mathbf{v}_0 \quad (2.29)$$

$$\text{with } \mathbf{H}_0 = [\mathbf{I}_{N_i} \quad -\mathbf{Z}_{OL}(\mathbf{Z}_{pass} + \mathbf{Z}_{LL})^{-1}],$$

and so we can reduce the system shown in Figure 2.5, to the system shown in Figure 2.4.

2.2.5 Signal Covariance Matrix

To calculate the achievable sum rate of the systems (c.f. Section 2.4), we need to derive the signal covariance matrix, defined as $\mathbb{E}[\mathbf{v}_L^s \mathbf{v}_L^{sH}]$.

We assume without loss of generality, that transmitter "0" is the corresponding partner of receiver "0". As in all the transfer functions from \mathbf{v}_0 to \mathbf{v}_L^s only impedance matrices appear, the covariance matrix becomes

$$\mathbf{K}_s = \mathbb{E}[\mathbf{v}_L^s \mathbf{v}_L^{sH}] = \mathbf{H}_{L,0} \cdot \mathbf{H}_0^{\text{sp}} \cdot \mathbb{E}[\mathbf{v}_0 \mathbf{v}_0^H] \cdot \mathbf{H}_0^{\text{sp}H} \cdot \mathbf{H}_{L,0}^H, \quad (2.30)$$

where $\mathbf{H}_{L,0}$ is the transfer function including any port reduction at the receiver and \mathbf{H}_0^{sp} the transferfunction over the spatial channel derived in Equation (2.2) for transmitter "0".

2.2.6 Interference Covariance Matrix

To calculate the interference covariance matrix, all the signal sources besides the partner (in this case, all but "0") have to be consider. This means, that all signal parts arriving at the loads of receiver "0" must be summed up over all the interferer. The interference covariance matrix hence becomes

$$\mathbf{K}_i = \mathbb{E}[\mathbf{v}_L^i \mathbf{v}_L^{iH}] = \sum_{j=1}^{N_{User}-1} \mathbf{H}_{L,0} \cdot \mathbf{H}_j^{\text{sp}} \cdot \mathbb{E}[\mathbf{v}_j \mathbf{v}_j^H] \cdot \mathbf{H}_j^{\text{sp}H} \cdot \mathbf{H}_{L,0}^H. \quad (2.31)$$

2.3 Noise Description

As mentioned in [3], there are four main noise sources in the receiver. In the following each noise source will be described and its transfer function towards the loads will be derived.

2.3.1 Antenna Noise

The antennas introduce two noise sources. The external noise \mathbf{n}_{ext} , collected from the radiation component of the antenna array and the noise generated by the losses in the antennas \mathbf{n}_l . From [4] it follows,

$$\mathbf{R}_{na} = \mathbb{E}[\mathbf{n}_{AR}\mathbf{n}_{AR}^H] = 4k_B B_W (T_{AE}\mathbb{R}\{\mathbf{Z}_{AR}\} + T_{AL}\mathbf{R}_{AR}), \quad (2.32)$$

with k_B the Boltzmann constant and B_W the bandwidth.

Transfer Function of the Antenna Noise

As the antenna noise is picked up by the antennas in the same way as the signal, the transfer function remains the same as the one derived in Section 2.2.3 for the signal, e.g.

$$\begin{aligned} \mathbf{H}_{L,0} &= \mathbf{H}_{L,LNA} \cdot \mathbf{H}_{LNA,M} \cdot \mathbf{H}_{M,0}, \quad \text{including port reduction} \\ \mathbf{H}_{L,0} &= \mathbf{H}_{L,LNA} \cdot \mathbf{H}_{LNA,M} \cdot \mathbf{H}_{M,0} \cdot \mathbf{H}_0. \end{aligned} \quad (2.33)$$

2.3.2 LNA Noise

The LNA introduces the third noise source. From the discussion in [1], the noise of the LNA is modeled by a series of voltages and parallel currents at the input of the LNA. The noise sources have the following statistical properties,

$$\begin{aligned} \mathbb{E}[\mathbf{i}_{LNA}\mathbf{i}_{LNA}^H] &= \beta \mathbf{I}_{N_r}, \\ \mathbb{E}[\mathbf{v}_{LNA}\mathbf{v}_{LNA}^H] &= \beta R_n^2 \mathbf{I}_{N_r}, \quad \text{and} \\ \mathbb{E}[\mathbf{v}_{LNA}\mathbf{i}_{LNA}^H] &= \rho \beta R_n \mathbf{I}_{N_r}, \end{aligned} \quad (2.34)$$

with ρ and β as correlation coefficients.

Transfer Function of the LNA Noise

As written above, we have two noise sources, the serial voltage sources and the parallel current sources. First we will transfer the current source into a voltage source in series as we then can use the same transfer function for the voltage and the transferred current sources. To do so, we need the equivalent input impedances looking from the left into the LNA block and from the right into the matching network. The equivalent input impedance for the LNA network \mathbf{Z}_{eqLNA_1} was already derived in (2.11). To get the equivalent input impedance for the matching network looking from the right into it we use Equation (2.5) and get

$$\tilde{\mathbf{Z}}_{eqM_2} = \mathbf{Z}_{M22} - \mathbf{Z}_{M12} \cdot (\mathbf{Z}_{M11} + \mathbf{Z}_{C'})^{-1} \cdot \mathbf{Z}_{M21}. \quad (2.35)$$

Transferring the current source into a series of voltages gives us

$$\mathbf{v}_{LNAc} = -\tilde{\mathbf{Z}}_{eqM_2} \mathbf{i}_{LNA}, \quad (2.36)$$

and therefore a transfer function of

$$\mathbf{H}_{L,LNA_v} = R_L \mathbf{I}_{N_r} (R_L \mathbf{I}_{N_r} + \tilde{\mathbf{Z}}_{eqLNA_2})^{-1} \mathbf{e} \cdot (\mathbf{c} + \tilde{\mathbf{Z}}_{eqM_2})^{-1}, \quad (2.37)$$

for the series voltages and

$$\mathbf{H}_{L,LNA_c} = -R_L \mathbf{I}_{N_r} (R_L \mathbf{I}_{N_r} + \tilde{\mathbf{Z}}_{eqLNA_2})^{-1} \mathbf{e} \cdot (\mathbf{c} + \tilde{\mathbf{Z}}_{eqM_2})^{-1} \tilde{\mathbf{Z}}_{eqM_2}, \quad (2.38)$$

for the LNA noise currents.

2.3.3 Downstream Noise

The last noise source is the downstream noise, generated by all the circuitry after the LNA [5] and modeled by voltage sources $\tilde{\mathbf{v}}_n$ in series to the loads. With the statistical property

$$\mathbb{E}[\tilde{\mathbf{v}}_n \tilde{\mathbf{v}}_n^H] = \psi \mathbf{I}_{N_r}. \quad (2.39)$$

Transfer Function of the Downstream Noise

For the transfer function of the downstream noise we need a simple voltage divider of the loads and the equivalent input impedance $\tilde{\mathbf{Z}}_{eqLNA_2}$ looking from the right into the LNA block. Note, that this is NOT the same input impedance as in (2.13). Therefore the transfer function becomes

$$\mathbf{H}_{L,n} = R_L \mathbf{I}_{N_r} (R_L \mathbf{I}_{N_r} + \tilde{\mathbf{Z}}_{eqLNA_2})^{-1}, \quad (2.40)$$

with

$$\tilde{\mathbf{Z}}_{eqLNA_2} = \mathbf{g} - \mathbf{d} \cdot (\mathbf{c} + \tilde{\mathbf{Z}}_{eqM_2})^{-1} \cdot \mathbf{e} = \mathbf{g}. \quad (2.41)$$

However, under the unilateral assumption the input impedance reduces to $\tilde{\mathbf{Z}}_{eqLNA_2} = \mathbf{g}$.

2.3.4 Noise Coupling

So far we transferred the noise from its source to the loads behind the LNA block. However additionally to the direct path, we need to take the noise of different receiver branches into account. Therefore we transfer the noise sources to series voltages next to the antenna voltages, so that we can use the transfer functions derived in Chapter 2.2.

As in the previous Section, we consider again the four noise types. For the antenna noise, we note, that we do not need to derive a transfer function. In a first step we transfer the LNA-current noise source and the downstream noise to the LNA-voltage noise source. Therefore the LNA-current noise source is multiplied by the equivalent input impedance of the LNA

$$\mathbf{v}_{LNAc} = \mathbf{Z}_{eqLNA_1} \mathbf{i}_{LNA}. \quad (2.42)$$

For the downstream noise we note, that under the unilateral assumption, the transferred noise is zero, else

$$\mathbf{v}_{LNA n} = \mathbf{d}(\mathbf{g} + R_L \mathbf{I}_{N_r})^{-1} \tilde{\mathbf{v}}_v. \quad (2.43)$$

Now we only need to find the transfer function for the LNA-voltage source $\mathbf{v}_{LNA v}$. The transfer function over the matching network is given by

$$\mathbf{H}_{0,LNA} = \mathbf{Z}_{M12}(\mathbf{Z}_{M22} + \mathbf{Z}_{eqLNA_1})^{-1}. \quad (2.44)$$

2.3.5 Noise Covariance Matrix

As in Chapter 2.2, we will derive the noise covariance matrix. To do so, we introduce the function $\Gamma(\cdot)$, which reshapes the matrices to our needs. For example Equation (2.44) must only be applied on the noise sources of the receivers, which shall be reduced, however a multiplication of the transfer matrix with the full noise

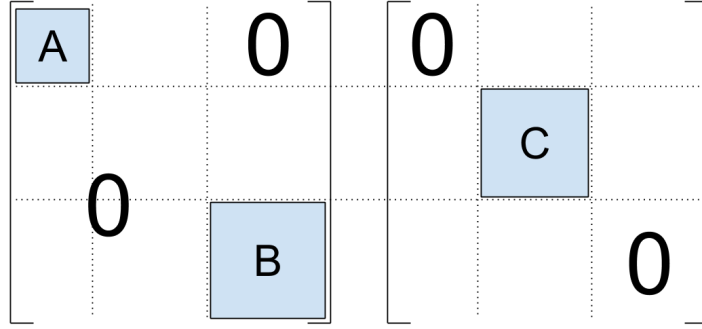


Figure 2.6: An example of the matrix shaping function. On the left the matrix shaped by $\Gamma(\cdot)$ on the right the matrix shaped by $\Gamma(\cdot)^{-1}$. The sub matrices **A**, **B** and **C** are square matrices and lie on the diagonal.

vector is desired. Let further $\Gamma(\cdot)^{-1}$, denote the function, which shapes the matrices only to the branches which are not reduced. We note the following properties of the function:

$$\begin{aligned} \Gamma(\mathbf{A}) \cdot \Gamma(\mathbf{B}) &= \Gamma(\mathbf{A} \cdot \mathbf{B}), \\ \Gamma(\mathbf{A}^H) &= \Gamma(\mathbf{A})^H, \\ \Gamma(\mathbf{A}) \cdot \Gamma(\mathbf{B})^{-1} &= \mathbf{0}, \quad \text{and} \\ \forall \mathbf{A}, \mathbf{B}, \quad &\text{which form a valid matrix multiplication } \mathbf{A} \cdot \mathbf{B}. \end{aligned} \quad (2.45)$$

Note that the first two properties are also valid for $\Gamma(\cdot)^{-1}$. Additionally for diagonal matrices the following property holds $\Gamma(\mathbf{A}) + \Gamma(\mathbf{A})^{-1} = \mathbf{A}$.

As we have multiple noise sources, first we will describe the noise output \mathbf{u}_L for each noise source, i.e.:

$$\begin{aligned} \mathbf{u}_{AR} &= \mathbf{H}_{L,0} \cdot \mathbf{n}_{AR}, \\ \mathbf{u}_{LNA_v} &= (\mathbf{H}_{L,0} \cdot \Gamma(\mathbf{H}_{0,LNA}) + \Gamma(\mathbf{H}_{L,LNA_v})^{-1}) \cdot \mathbf{v}_{LNA}, \\ \mathbf{u}_{LNA_c} &= (\mathbf{H}_{L,0} \cdot \Gamma(\mathbf{H}_{0,LNA} \mathbf{Z}_{eqLNA_1}) + \Gamma(\mathbf{H}_{L,LNA_c})^{-1}) \cdot \mathbf{i}_{LNA}, \\ \mathbf{u}_{\tilde{n}} &= (\mathbf{H}_{L,0} \cdot \Gamma(\mathbf{H}_{0,LNA} \cdot \mathbf{d}(\mathbf{g} + R_L \mathbf{I}_{N_R})^{-1}) + \Gamma(\mathbf{H}_{L,n})^{-1}) \cdot \tilde{\mathbf{v}}_n, \\ \text{and therefore } \mathbf{u}_L &= \mathbf{u}_{AR} + \mathbf{u}_{LNA_v} + \mathbf{u}_{LNA_c} + \mathbf{u}_{\tilde{n}}. \end{aligned} \quad (2.46)$$

Because all the noise sources are uncorrelated, except for the LNA noise sources (Equation (??)), the noise covariance matrix can be written as:

$$\begin{aligned} \mathbf{K}_n = \mathbb{E}[\mathbf{u}_L \mathbf{u}_L^H] &= \mathbf{H}_{L,0} \mathbb{E}[\mathbf{n}_{AR} \mathbf{n}_{AR}^H] \mathbf{H}_{L,0}^H + \mathbb{E}[\mathbf{u}_{LNA_v} \mathbf{u}_{LNA_v}^H] + \mathbb{E}[\mathbf{u}_{LNA_v} \mathbf{u}_{LNA_c}^H] + \\ &\quad \mathbb{E}[\mathbf{u}_{LNA_c} \mathbf{u}_{LNA_v}^H] + \mathbb{E}[\mathbf{u}_{LNA_c} \mathbf{u}_{LNA_c}^H] + \mathbb{E}[\mathbf{u}_{\tilde{n}} \mathbf{u}_{\tilde{n}}^H] \end{aligned} \quad (2.47)$$

For simplicity reasons, we will look in every summand separately in the following. As $-\mathbf{H}_{L,LNA_v} \cdot \tilde{\mathbf{Z}}_{eqM_2} = \mathbf{H}_{L,LNA_c}$ and using (2.32), (2.34), (2.39) and (2.45), it

follows

$$\begin{aligned}
\mathbf{K}_{n_{LNA_{vv}}} &= \mathbb{E} \left[(\mathbf{H}_{L,0} \cdot \Gamma(\mathbf{H}_{0,LNA}) + \Gamma(\mathbf{H}_{L,LNA_v})^{-1}) \cdot \mathbf{v}_{LNA} \mathbf{v}_{LNA}^H \cdot \right. \\
&\quad \left. (\mathbf{H}_{L,0} \cdot \Gamma(\mathbf{H}_{0,LNA}) + \Gamma(\mathbf{H}_{L,LNA_v})^{-1})^H \right] \\
&= (\mathbf{H}_{L,0} \cdot \Gamma(\mathbf{H}_{0,LNA}) + \Gamma(\mathbf{H}_{L,LNA_v})^{-1}) \cdot \mathbb{E} [\mathbf{v}_{LNA} \mathbf{v}_{LNA}^H] \cdot \\
&\quad (\mathbf{H}_{L,0} \cdot \Gamma(\mathbf{H}_{0,LNA}) + \Gamma(\mathbf{H}_{L,LNA_v})^{-1})^H \\
&= \beta R_n^2 \left(\mathbf{H}_{L,0} \cdot \Gamma(\mathbf{H}_{0,LNA} \mathbf{H}_{0,LNA}^H) \mathbf{H}_{0,LNA}^H + \Gamma(\mathbf{H}_{L,LNA_v} \mathbf{H}_{L,LNA_v}^H)^{-1} \right), \tag{2.48}
\end{aligned}$$

for the LNA-voltage source and

$$\begin{aligned}
\mathbf{K}_{n_{LNA_{cc}}} &= \beta \left(\mathbf{H}_{L,0} \cdot \Gamma(\mathbf{H}_{0,LNA} \mathbf{Z}_{eqLNA_1} \mathbf{Z}_{eqLNA_1}^H \mathbf{H}_{0,LNA}^H) \mathbf{H}_{0,LNA}^H + \right. \\
&\quad \left. \Gamma(\mathbf{H}_{L,LNA_v} \tilde{\mathbf{Z}}_{eqM_2} \tilde{\mathbf{Z}}_{eqM_2}^H \mathbf{H}_{L,LNA_v}^H)^{-1} \right), \tag{2.49}
\end{aligned}$$

for the LNA-current source. For the cross terms it follows

$$\begin{aligned}
\mathbf{K}_{n_{LNA_{vc}}} &= \rho \beta R_n \left(\mathbf{H}_{L,0} \cdot \Gamma(\mathbf{H}_{0,LNA} \mathbf{Z}_{eqLNA_1}^H \mathbf{H}_{0,LNA}^H) \mathbf{H}_{L,0}^H + \Gamma(\mathbf{H}_{L,LNA_v} \tilde{\mathbf{Z}}_{eqM_2}^H \mathbf{H}_{L,LNA_v}^H)^{-1} \right) \\
&\quad + \rho^* \beta R_n \left(\mathbf{H}_{L,0} \cdot \Gamma(\mathbf{H}_{0,LNA} \mathbf{Z}_{eqLNA_1} \mathbf{H}_{0,LNA}^H) \mathbf{H}_{L,0}^H + \Gamma(\mathbf{H}_{L,LNA_v} \tilde{\mathbf{Z}}_{eqM_2} \mathbf{H}_{L,LNA_v}^H)^{-1} \right) \\
&= 2\beta R_n \left(\mathbf{H}_{L,0} \cdot \Gamma(\mathbf{H}_{0,LNA} \mathbb{R}\{\rho^* \mathbf{Z}_{eqLNA_1}\} \mathbf{H}_{0,LNA}^H) \mathbf{H}_{L,0}^H + \right. \\
&\quad \left. \Gamma(\mathbf{H}_{L,LNA_v} \mathbb{R}\{\rho^* \tilde{\mathbf{Z}}_{eqM_2}\} \mathbf{H}_{L,LNA_v}^H)^{-1} \right), \tag{2.50}
\end{aligned}$$

and for the downstream noise

$$\begin{aligned}
\mathbf{K}_{n_{\tilde{n}\tilde{n}}} &= \psi(\mathbf{H}_{L,0} \cdot \Gamma(\mathbf{H}_{0,\tilde{n}}) + \Gamma(\mathbf{H}_{L,\tilde{n}})^{-1}) \cdot (\Gamma(\mathbf{H}_{0,\tilde{n}})^H \cdot \mathbf{H}_{L,0}^H + \Gamma(\mathbf{H}_{L,\tilde{n}}^H)^{-1}) \\
&= \psi(\mathbf{H}_{L,0} \cdot \Gamma(\mathbf{H}_{0,\tilde{n}} \mathbf{H}_{0,\tilde{n}}^H) \cdot \mathbf{H}_{L,0}^H + \Gamma(\mathbf{H}_{L,\tilde{n}} \mathbf{H}_{L,\tilde{n}}^H)^{-1}). \tag{2.51}
\end{aligned}$$

With these results we can form the final noise covariance matrix as

$$\mathbf{K}_n = \mathbf{H}_{L,0} \mathbb{E}[\mathbf{n}_{AR} \mathbf{n}_{AR}^H] \mathbf{H}_{L,0}^H + \mathbf{K}_{n_{LNA_{vv}}} + \mathbf{K}_{n_{LNA_{cc}}} + \mathbf{K}_{n_{LNA_{vc}}} + \mathbf{K}_{n_{\tilde{n}\tilde{n}}}. \tag{2.52}$$

2.4 Rate Calculations

TO-DO

Chapter 3

Analytical Gradient

In the following the derivation of the gradients will be given. In the first section the signal gradients will be derived, in the later the noise gradients. The gradients are derived to improve the achievable sum rate function of the system. It is given by

$$\begin{aligned} r &= \log_2 (\det (\mathbf{K}_s \mathbf{K}_i^{-1} \mathbf{K}_n^{-1} + \mathbf{I}_{N_r})) \\ &= \log_2 (\det (\mathbf{K}_s + \mathbf{K}_i + \mathbf{K}_n)) - \log_2 (\det (\mathbf{K}_i + \mathbf{K}_n)), \end{aligned} \quad (3.1)$$

where \mathbf{K}_s , \mathbf{K}_i and \mathbf{K}_n denote the signal, interference and noise covariance matrices derived in (2.30), (2.31) and (2.52).

We are interested in the gradient of the achievable sum rate with respect to the matching network and the passive antenna loads. Using the matrix relations from [6] the gradient becomes

$$\begin{aligned} \frac{\partial r}{\partial \mathbf{Z}_{l,ij}} &= \frac{1}{\ln(2)} \text{Tr} \left((\mathbf{K}_s + \mathbf{K}_i + \mathbf{K}_n)^{-1} \left(\frac{\partial \mathbf{K}_s}{\partial \mathbf{Z}_{l,ij}} + \frac{\partial \mathbf{K}_i}{\partial \mathbf{Z}_{l,ij}} + \frac{\partial \mathbf{K}_n}{\partial \mathbf{Z}_{l,ij}} \right) - \right. \\ &\quad \left. (\mathbf{K}_i + \mathbf{K}_n)^{-1} \left(\frac{\partial \mathbf{K}_i}{\partial \mathbf{Z}_{l,ij}} + \frac{\partial \mathbf{K}_n}{\partial \mathbf{Z}_{l,ij}} \right) \right), \end{aligned} \quad (3.2)$$

with $l \in \{11, 12, 22, \text{pass}\}$ denoting the sub-matrices of the matching network or the passive antenna loads and i, j denoting the element in the i -th row and j -th column. In the following the gradient is split up in the signal and the noise part. The derivatives for each covariance matrix will be derived.

3.1 Signal Gradient

For the signal covariance matrix, we see from Equation (2.30), that we can take the derivative of each sub transfer function and place them together afterwards by the chain rule. First of all, we check which sub transfer functions are affected by the gradient. We see that for the matching network sub matrices, we need to take the derivative of the transfer functions $\mathbf{H}_{LNA,M}$ and $\mathbf{H}_{M,0}$. For the passive antenna loads \mathbf{Z}_{pass} obviously \mathbf{H}_0 for the port reduction is affected. Additionally $\mathbf{H}_{M,0}$ is affected because it contains $\mathbf{Z}_{C'}$.

For the following \mathbf{J}_{ij} denotes the single entry matrix, with respect to the i -th row and the j -th column. It follows for the port reduction transfer function

$$\frac{\partial \mathbf{H}_0}{\partial \mathbf{Z}_{\text{pass},ij}} = [\mathbf{0}_{N_i} \quad \mathbf{Z}_{OL}(\mathbf{Z}_{\text{pass}} + \mathbf{Z}_{LL})^{-1} \mathbf{J}_{ij}(\mathbf{Z}_{\text{pass}} + \mathbf{Z}_{LL})^{-1}] \quad (3.3)$$

with $\mathbf{0}_{N_i}$ the N_i by N_i all-zeros matrix. For the voltage divider before the matching network it follows,

$$\frac{\partial \mathbf{H}_{M,0}}{\partial \mathbf{Z}_{11,ij}} = \mathbf{J}_{ij}(\mathbf{Z}_{eqM_1} + \mathbf{Z}_{C'})^{-1} - \mathbf{Z}_{eqM_1}(\mathbf{Z}_{eqM_1} + \mathbf{Z}_{C'})^{-1} \mathbf{J}_{ij}(\mathbf{Z}_{eqM_1} + \mathbf{Z}_{C'})^{-1}, \quad (3.4)$$

$$\begin{aligned} \text{with } \frac{\partial \mathbf{Z}_{eqM_1}}{\partial \mathbf{Z}_{M12}} &= \mathbf{J}_{ij}^T(\mathbf{Z}_{M22} + \mathbf{Z}_{eqLNA_1})^{-1} \mathbf{Z}_{M12} + \mathbf{Z}_{M12}^T(\mathbf{Z}_{M22} + \mathbf{Z}_{eqLNA_1})^{-1} \mathbf{J}_{ij}, \\ \frac{\partial \mathbf{H}_{M,0}}{\partial \mathbf{Z}_{12,ij}} &= \frac{\partial \mathbf{Z}_{eqM_1}}{\partial \mathbf{Z}_{M12}}(\mathbf{Z}_{eqM_1} + \mathbf{Z}_{C'})^{-1} - \mathbf{Z}_{eqM_1}(\mathbf{Z}_{eqM_1} + \mathbf{Z}_{C'})^{-1} \frac{\partial \mathbf{Z}_{eqM_1}}{\partial \mathbf{Z}_{M12}}(\mathbf{Z}_{eqM_1} + \mathbf{Z}_{C'})^{-1}, \end{aligned} \quad (3.5)$$

$$\begin{aligned} \text{with } \frac{\partial \mathbf{Z}_{eqM_1}}{\partial \mathbf{Z}_{M22}} &= \mathbf{Z}_{M12}^T(\mathbf{Z}_{M22} + \mathbf{Z}_{eqLNA_1})^{-1} \mathbf{J}_{ij}^T(\mathbf{Z}_{M22} + \mathbf{Z}_{eqLNA_1})^{-1} \mathbf{Z}_{M12}, \\ \frac{\partial \mathbf{H}_{M,0}}{\partial \mathbf{Z}_{22,ij}} &= \frac{\partial \mathbf{Z}_{eqM_1}}{\partial \mathbf{Z}_{M22}}(\mathbf{Z}_{eqM_1} + \mathbf{Z}_{C'})^{-1} - \mathbf{Z}_{eqM_1}(\mathbf{Z}_{eqM_1} + \mathbf{Z}_{C'})^{-1} \frac{\partial \mathbf{Z}_{eqM_1}}{\partial \mathbf{Z}_{M22}}(\mathbf{Z}_{eqM_1} + \mathbf{Z}_{C'})^{-1}, \end{aligned} \quad (3.6)$$

$$\begin{aligned} \text{and with } \frac{\partial \mathbf{Z}_{C'}}{\partial \mathbf{Z}_{\text{pass},ij}} &= \mathbf{Z}_{OL}(\mathbf{Z}_{\text{pass}} + \mathbf{Z}_{LL})^{-1} \mathbf{J}_{ij}(\mathbf{Z}_{\text{pass}} + \mathbf{Z}_{LL})^{-1} \mathbf{Z}_{LO} \\ \frac{\partial \mathbf{H}_{M,0}}{\partial \mathbf{Z}_{\text{pass},ij}} &= -\mathbf{Z}_{eqM_1}(\mathbf{Z}_{eqM_1} + \mathbf{Z}_{C'})^{-1} \frac{\partial \mathbf{Z}_{C'}}{\partial \mathbf{Z}_{\text{pass},ij}}(\mathbf{Z}_{eqM_1} + \mathbf{Z}_{C'})^{-1}. \end{aligned} \quad (3.7)$$

Last, the transfer function over the matching network is affected as follows

$$\frac{\partial \mathbf{H}_{LNA,M}}{\partial \mathbf{Z}_{11,ij}} = -\mathbf{H}_{LNA,M} \mathbf{J}_{ij} \mathbf{Z}_{M11}^{-1} \mathbf{Z}_{M12}(\mathbf{Z}_{eqLNA_1} + \mathbf{Z}_{eqM_2})^{-1} \mathbf{Z}_{M12} \mathbf{Z}_{M11}^{-1} - \mathbf{H}_{LNA,M} \mathbf{J}_{ij} \mathbf{Z}_{M11}^{-1} \quad (3.8)$$

$$\begin{aligned} \frac{\partial \mathbf{H}_{LNA,M}}{\partial \mathbf{Z}_{12,ij}} &= \mathbf{Z}_{eqLNA_1}(\mathbf{Z}_{eqLNA_1} + \mathbf{Z}_{eqM_2})^{-1} (-\mathbf{J}_{ij}^T \mathbf{Z}_{M11}^{-1} \mathbf{Z}_{M12} - \mathbf{Z}_{M12}^T \mathbf{Z}_{M11}^{-1} \mathbf{J}_{ij}) \cdot \\ &\quad (\mathbf{Z}_{eqLNA_1} + \mathbf{Z}_{eqM_2})^{-1} \mathbf{Z}_{M12} \mathbf{Z}_{M11}^{-1} + \mathbf{Z}_{eqLNA_1}(\mathbf{Z}_{eqLNA_1} + \mathbf{Z}_{eqM_2})^{-1} \mathbf{J}_{ij} \mathbf{Z}_{M11}^{-1}, \end{aligned} \quad (3.9)$$

$$\frac{\partial \mathbf{H}_{LNA,M}}{\partial \mathbf{Z}_{22,ij}} = \mathbf{Z}_{eqLNA_1}(\mathbf{Z}_{eqLNA_1} + \mathbf{Z}_{eqM_2})^{-1} \mathbf{J}_{ij}(\mathbf{Z}_{eqLNA_1} + \mathbf{Z}_{eqM_2})^{-1} \mathbf{Z}_{M12} \mathbf{Z}_{M11}^{-1} \quad (3.10)$$

With these derivations, we can apply the chain rule on the transfer function in (??) to get $\frac{\partial \mathbf{K}_s}{\partial \mathbf{Z}_{L,ij}}$.

3.2 Interference Gradient

TO-DO

3.3 Noise Gradients

As written in Section ??, we have four noise sources. Because they sum up at the loads after the LNA, we can look at each noise transfer function separately and analyze it on its own.

3.3.1 Antenna Noise Gradient

As the antenna noise is picked up at the same place as the signal, its gradient is also the same as the signal covariance gradient. The formulas from (3.3) to (3.15)

apply in the same manner to the antenna noise transfer functions. Therefore they are omitted here. We only note, that the transfer functions \mathbf{H}_0 , $\mathbf{H}_{M,0}$ and $\mathbf{H}_{LNA,M}$ are affected in the derivation of $\frac{\partial \mathbf{K}_n}{\partial \mathbf{Z}_{l,ij}}$, with $l \in \{11, 12, 22, \text{pass}\}$.

3.3.2 LNA Noise Gradient

Looking at the transfer function of the two LNA noise sources, we see that neither $\mathbf{H}_{L,LNA}$ nor \mathbf{Z}_{eqLNA_1} are affected by the derivations. Only $\tilde{\mathbf{Z}}_{eqM_2}$ and therefore \mathbf{H}_{L,LNA_v} have to be taken into account. It follows,

$$\frac{\partial \tilde{\mathbf{Z}}_{eqM_2}}{\partial \mathbf{Z}_{11,ij}} = \mathbf{Z}_{M12}(\mathbf{Z}_{M11} + \mathbf{Z}_{C'})^{-1} \mathbf{J}_{ij}(\mathbf{Z}_{M11} + \mathbf{Z}_{C'})^{-1}, \quad (3.11)$$

$$\frac{\partial \tilde{\mathbf{Z}}_{eqM_2}}{\partial \mathbf{Z}_{12,ij}} = -\mathbf{J}_{ij}(\mathbf{Z}_{M11} + \mathbf{Z}_{C'})^{-1} \mathbf{Z}_{M21} - \mathbf{Z}_{M12}(\mathbf{Z}_{M11} + \mathbf{Z}_{C'})^{-1} \mathbf{J}_{ij}^T, \quad (3.12)$$

$$\frac{\partial \tilde{\mathbf{Z}}_{eqM_2}}{\partial \mathbf{Z}_{22,ij}} = \mathbf{J}_{ij}, \quad (3.13)$$

and with $\frac{\partial \mathbf{Z}_{C'}}{\partial \mathbf{Z}_{\text{pass},ij}} = \mathbf{Z}_{OL}(\mathbf{Z}_{\text{pass}} + \mathbf{Z}_{LL})^{-1} \mathbf{J}_{ij}(\mathbf{Z}_{\text{pass}} + \mathbf{Z}_{LL})^{-1} \mathbf{Z}_{LO}$,

$$\frac{\partial \tilde{\mathbf{Z}}_{eqM_2}}{\partial \mathbf{Z}_{\text{pass},ij}} = \mathbf{Z}_{M12}(\mathbf{Z}_{M11} + \mathbf{Z}_{C'})^{-1} \frac{\partial \mathbf{Z}_{C'}}{\partial \mathbf{Z}_{\text{pass},ij}} (\mathbf{Z}_{M11} + \mathbf{Z}_{C'})^{-1} \mathbf{Z}_{M21}, \quad (3.14)$$

which results in

$$\frac{\mathbf{H}_{L,LNA_v}}{\partial \mathbf{Z}_{l,ij}} = -\mathbf{H}_{L,LNA} \mathbf{Z}_{eqLNA_1} (\mathbf{Z}_{eqLNA_1} + \tilde{\mathbf{Z}}_{eqM_2})^{-1} \frac{\partial \tilde{\mathbf{Z}}_{eqM_2}}{\partial \mathbf{Z}_{l,ij}} (\mathbf{Z}_{eqLNA_1} + \tilde{\mathbf{Z}}_{eqM_2})^{-1}. \quad (3.15)$$

3.3.3 Downstream Noise Gradient

Last, we see, that the transfer function of the downstream noise $\mathbf{H}_{L,\tilde{n}}$ is not affected by any of the derivations above under the unilateral assumption. Otherwise, $\tilde{\mathbf{Z}}_{eqLNA_2}$ is a function of the matching network and the passive antenna loads. It follows,

3.3.4 Noise Gradient

We can now write the gradient of the noise covariance matrix as

$$\begin{aligned} \frac{\partial \mathbf{K}_n}{\partial \mathbf{Z}_{l,ij}} &= \frac{\partial \mathbf{H}_{L,0}}{\partial \mathbf{Z}_{l,ij}} \mathbf{R}_{na} \mathbf{H}_{L,0}^H + \mathbf{H}_{L,0} \mathbf{R}_{na} \frac{\partial \mathbf{H}_{L,0}}{\partial \mathbf{Z}_{l,ij}}^H \\ &\quad + \frac{\partial \mathbf{H}_{L,LNA_v}}{\partial \mathbf{Z}_{l,ij}} \beta \left(R_N^2 \mathbf{I}_{N_r} - 2R_N \mathbb{R}\{\rho^* \tilde{\mathbf{Z}}_{eqM_2}\} + \tilde{\mathbf{Z}}_{eqM_2} \tilde{\mathbf{Z}}_{eqM_2}^H \right) \mathbf{H}_{L,LNA_v}^H + \\ &\quad + \mathbf{H}_{L,LNA_v} \beta \left(2R_N \frac{\partial \mathbb{R}\{\rho^* \tilde{\mathbf{Z}}_{eqM_2}\}}{\partial \mathbf{Z}_{l,ij}} + \frac{\partial \tilde{\mathbf{Z}}_{eqM_2}}{\partial \mathbf{Z}_{l,ij}} \tilde{\mathbf{Z}}_{eqM_2}^H + \tilde{\mathbf{Z}}_{eqM_2} \left(\frac{\partial \tilde{\mathbf{Z}}_{eqM_2}}{\partial \mathbf{Z}_{l,ij}} \right)^H \right) \mathbf{H}_{L,LNA_v}^H + \\ &\quad + \mathbf{H}_{L,LNA_v} \beta \left(R_N^2 \mathbf{I}_{N_r} - 2R_N \mathbb{R}\{\rho^* \tilde{\mathbf{Z}}_{eqM_2}\} + \tilde{\mathbf{Z}}_{eqM_2} \tilde{\mathbf{Z}}_{eqM_2}^H \right) \frac{\partial \mathbf{H}_{L,LNA_v}}{\partial \mathbf{Z}_{l,ij}}^H. \end{aligned} \quad (3.16)$$

Chapter 4

Problem Statement and Solver Methods

In the following, the problem to optimize will be introduced and analyzed. Although the thesis is not looking into finding the optimal solution, different solver strategies have to be introduced and compared to each other, as the utility function is not trivial and the differences are severe. Their advantages and disadvantages will be shown. If not specifically mentioned, we will look at a 2x2 MIMO system with one receive antenna per user and three relays, as shown in Figure ???. The relays in this system will be lossless, i.e. the impedances will be pure imaginary.

4.1 Utility Function

As the aim for wireless communication networks is to maximize the achievable rate, we take the formulas derived in Section 2.4, which describe the rates for each transmit-receive pair. In order to get an utility function from the achievable rates, we stack them into the vector $\mathbf{r} = [r_1 \ r_2 \ \dots \ r_N]^T$. To optimize the rates, different approaches are possible.

- Optimize the minimum rate, i.e. $\max(\min(\mathbf{r}))$ (maxmin),
- Optimize the mean rate, i.e. $\max(\sum(\mathbf{r}))$ (maxsum), and
- Optimize the maximum rate, i.e. $\max(\max(\mathbf{r}))$ (maxmax).

This is done using the LP-norm ($\|\mathbf{r}\|_p$) [7]. By setting $p = -\text{Inf}$, the "maxmin" method is achieved. Setting $p = 1$, the "maxsum" method is applied and setting $p = +\text{Inf}$, the "maxmax" method is applied. For all values in between, the utility function "tends" to optimize the maximum and minimum value respectively.

In the following we restrict ourselves to the "maxsum" method. As the other methods easily can be applied and will lead to a similarly good result without loss of generality.

4.1.1 Convexity of the Utility Function

In the following the convexity of the utility function is analyzed. This is done, because the choice of the solver depends on the shape of the utility function (e.g. in case of a concave utility function, a normal gradient search is sufficient to provide good results).

To do so, we analyze the utility function at different input values for the passive relays and at different input power values. It is clear, that the function changes

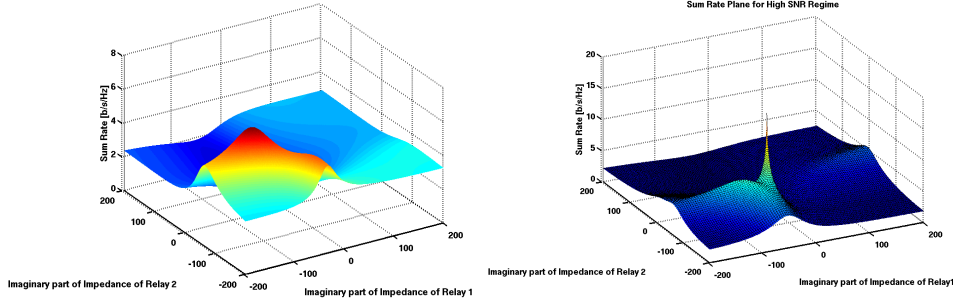


Figure 4.1: The utility function for different imaginary relay impedances for two relays and two different channel realizations.

(heavily) for every channel realization. Figure 4.1 shows two different channel realizations for the same input power and the same domain of two passive impedances.

4.1.2 Dependency on the Input Power

We will analyze now the utility function for different input powers. In Figure ?? and Figure ?? we see the same channel realization for two different input powers. Figure ?? shows again the same channel realization at an input power close to the input power of Figure ??.

First we observe, that the optima in Figure ?? and Figure ?? lie at very different impedance values of the relays, therefore we can conclude, that an optimal solution for one input power does not necessarily lead to a good solution for a different input power solution.

Next we analyze the optima of Figure ?? and Figure ?. Here we can see again, that using the values from Figure ?? in Figure ?? will not lead to the best solution, however it would serve as a good initial value for a gradient search method.

4.1.3 Difference of Local Optima

Last, we want to look at the local optima we can possibly run into. We see in Figure ??, that if we hit the local optimum at the left, the performance will be nearly the same as with the local optimum at the right. However looking at Figure ??, we see that the difference of the local optimum before the peak and the peak itself is severe. Therefore, we can not only try to run the optimization with one initialization, but instead, we need multiple initializations.

4.1.4 Complexity of the Problem

As we will discuss different solver approaches in the following Sections, a short description of the complexity of the problem is given. For each relay we use, we will have one variable (N_{Rel}), if we restrict the relays to the imaginary domain. Allowing the relay to become lossy and therefore the impedance complex, the number of variables is doubled. Further for each receiver branch, i.e. receiver antenna, we have a reciprocal (lossless) matching network (see Section ??), which has to be optimized. Therefore we have three elements per branch (in total: $3 \cdot N_{\text{R}} \cdot N_{\text{Rx}}$). For a four user MIMO system with two receive antennas and five lossy relays per user, this would lead to a problem of size $N_{\text{var}} = 2 \cdot 4 \cdot 5 + 3 \cdot 4 \cdot 2 = 64$. As mentioned in the beginning

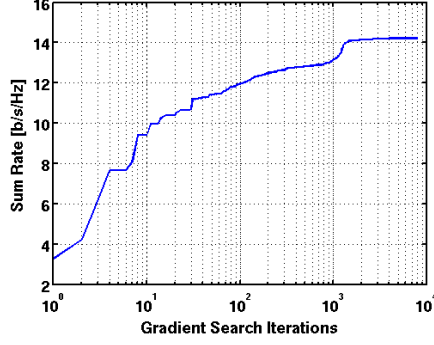


Figure 4.2: The sum rate over the gradient search iterations.

of this chapter, we look at a 2x2 MIMO system with one receive antenna and three lossless relays. The complexity of this system is therefore $N_{\text{var}} = 1 \cdot 2 \cdot 3 + 3 \cdot 2 \cdot 1 = 12$.

4.2 Gradient Search

Despite this large number of variables and the non-convexity of the utility function, the first approach remains a gradient search. Figure 4.2 shows the typical behaviour of the gradient search for a realization over the iteration steps. In the following, different methods are described, to improve the algorithm.

4.2.1 Choice of Initial Values

We try to overcome the non-pleasant properties of the problem with a larger number of initial guesses, so that the gradient search approach tends more towards a grid search optimization method. The gradient search routine itself is then used as a refinement step of the grid search.

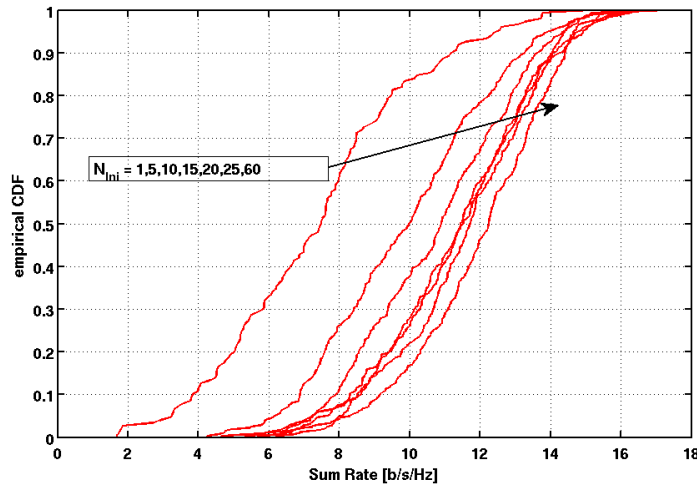


Figure 4.3: Comparison of the number of initial values used.

Figure 4.3 shows the empirical CDFs of the optimized sum rate, for different numbers of initializations. The initial values were drawn uniformly at random for

$Z_{\text{Rel}}[i] \in [-600, 600]j, \quad \forall i \in [1, N_{\text{Rel}}]$.

It is obvious and clear to see, that the larger the number of initializations, the better the result. However, even with 25 and 60 initializations, there improvement is still immense, which shows, that the number of initializations must be a lot larger than twice the input vector length. A good tradeoff between a decent optimization and a comparable small runtime of the optimization is achieved by a choice of four times the input vector length.

4.2.2 Adaptive Step Size

The performance of the gradient search routine is improved by the use of an adaptive step size. For each calculated gradient, the step taken into the direction of the gradient is increased until the new rate value is smaller than the previous calculated value as shown in Figure 4.4. Therefore the number of time-expensive gradient calculations is reduced immense.

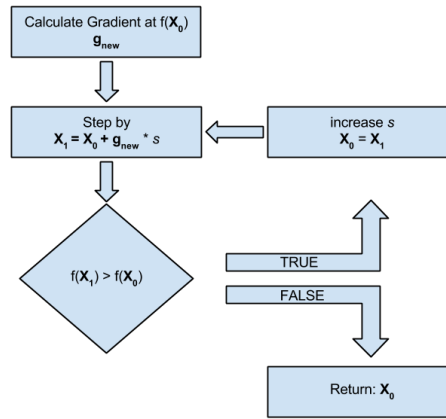


Figure 4.4: Schematic of the adaptive step size algorithm.

4.2.3 Conjugate Gradient

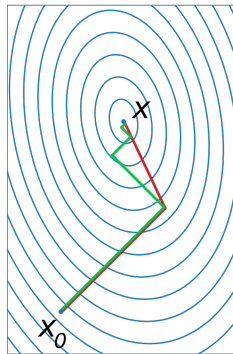


Figure 4.5: A comparison of the convergence of gradient descent with optimal step size (in green) and conjugate vector (in red) for minimizing a quadratic function associated with a given linear system[8].

As the gradient search performance still requires too many iterations, further improvements were made. The shape of such complex problems can - in some cases

- have the shape of a crest, where, with a unpleasant choice of the initial value, a pure gradient search routine might jump around the optimum, without improving a lot. Conjugate gradient routines like "Fletcher-Reeves" or "Polak-Ribière" lead to a faster convergence, as they weight the gradient by the previous gradient and a weight factor β .

Like Polak-Ribière, the Fletcher-Reeves method updates the conjugate direction according to

$$\mathbf{s}_n = \mathbf{g}_n + \beta_n \cdot \mathbf{g}_{n-1}, \quad (4.1)$$

where \mathbf{g} denotes the gradient. The conjugate direction \mathbf{s} is then used to perform the conjugate gradient search. Polak-Ribière and Fletcher-Reeves differ in the way, they calculate the weight factor β .

Fletcher-Reeves

For the method of Fletcher-Reeves, β is calculated according to [9]

$$\beta_n^{FR} = \frac{\mathbf{g}_n^T \mathbf{g}_n}{\mathbf{g}_{n-1}^T \mathbf{g}_{n-1}}. \quad (4.2)$$

Polak-Ribière

For the method of Polak-Ribière, β is calculated according to [10]

$$\beta_n^{PR} = \frac{\mathbf{g}_n^T (\mathbf{g}_n - \mathbf{g}_{n-1})}{\mathbf{g}_{n-1}^T \mathbf{g}_{n-1}}. \quad (4.3)$$

In Figure 4.6 the pure gradient search (steepest ascent) method is compared to the methods of Fletcher Reeves and Polak-Ribière. The Figure shows once the optimization after 50 iterations (solid lines), to see, which method optimizes the problem the best after just a few steps, and at 500 iterations, to see which routine might get caught in the shape of the problem.

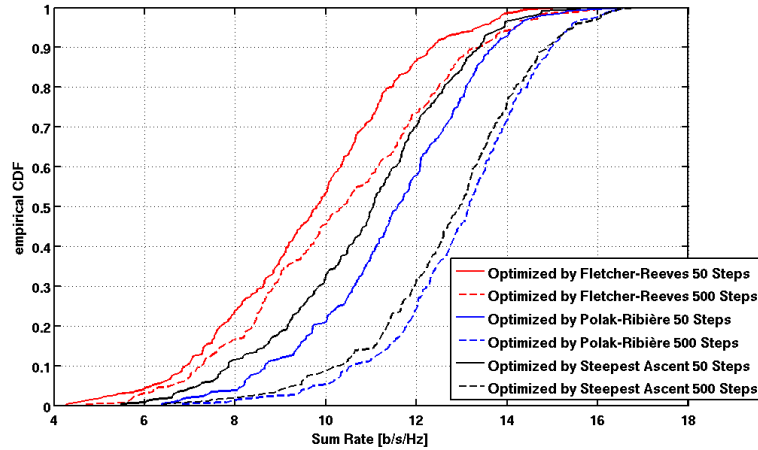


Figure 4.6: Comparison between Steepest Ascent, Polak-Ribière, and Fletcher-Reeves.

We can see, that Fletcher-Reeves is not well suited for our kind of optimization problem. Better is Polak-Ribière, which outperforms the standard gradient search method at 50 iterations and has a slightly better performance at 500 iterations.

4.3 Heuristic Optimization Algorithms

Due to the non convexity and the non trivial optimization problem, we further analyze (some) heuristic optimization methods. In the following three heuristic algorithms will be introduced and analyzed by their performance. They were chosen, because they already exist in the MATLAB library and do not require any strenuous implementation.

4.3.1 Simulated Annealing

Simulated Annealing was developed, as there is a deep and useful connection between statistical mechanics (the behavior of systems with many degrees of freedom in thermal equilibrium at a finite temperature) and multivariate or combinatorial optimization (finding the minimum of a given function depending on many parameters) [11]. In this thesis, Simulated Annealing was chosen as it is a method to solve optimization problems of multivariate optimization.

The Algorithm used in this thesis is a build-in function of MATLAB®. A description can be found on the MathWorks homepage [12].

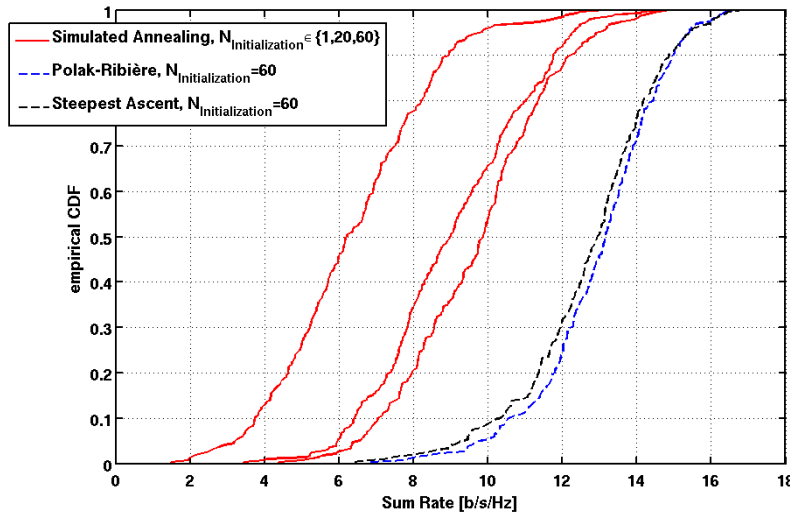


Figure 4.7: Comparison of the Simulated Annealing algorithm for different number of initializations and the results from "Polak-Ribière" and "Steepest Ascent" gradient searches.

Figure 4.7 shows the performance of Simulated Annealing algorithm dependent on the choice of numbers of initializations (red curves). Again we see, that the more initializations we have, the better the sum rate can be optimized. However, we also see, that even with 60 initializations, Simulated Annealing leads to a result, which is worse than the sum rates achieved by steepest ascent (black dashed curve) and Polak-Ribière (blue dashed curve).

4.3.2 GlobalSearch

The other two heuristic optimization algorithms are GlobalSearch (GS) and MultiStart (MS). They are very similar to each other, the only difference is the choice of the starting values. As MultiStart requires the number of initialization values,

GlobalSearch generates trial points on its own [13]. GlobalSearch - the optimization function, which we will analyze - is based on the MATLAB©built-in function *fmincon*. Figure 4.8 shows the schematics of GS and MS.

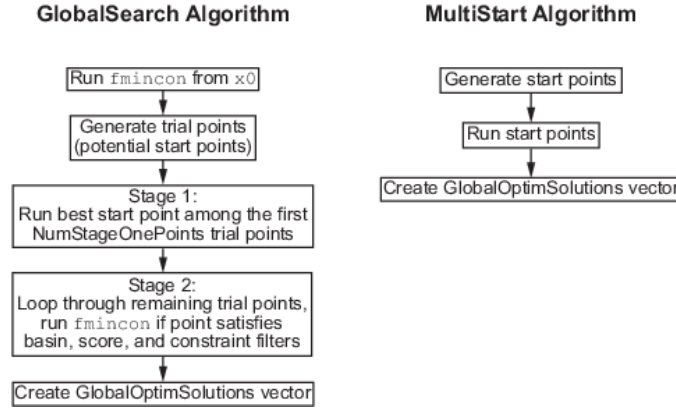


Figure 4.8: Schematics of the GlobalSearch and MultiStart algorithms [13].

Figure 4.9 shows the performance of GlobalSearch (red curve). We see, that it has almost the same performance as the conjugate gradient method by Polak-Ribière with 60 initializations (blue curve). GlobalSearch is less dependent on the initial value - for the relays it is chosen very large ($\mathbf{X}_{\text{Rel}} = 1000j$) and not at random, compared to the gradient search methods, to simulate an open circuited antenna and therefore no coupling.

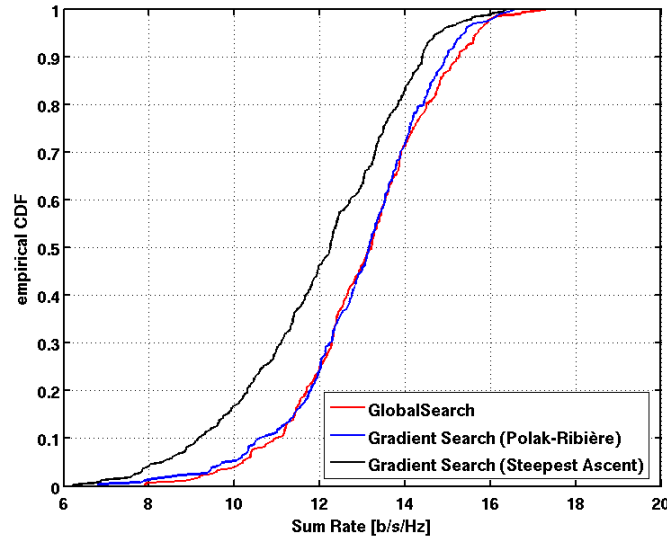


Figure 4.9: Performance of the GlobalSearch algorithm in comparison to the previous results.

4.4 Further Algorithm Improvements

4.4.1 Optimization of the Interference Function

A further approach to optimize the gradient search routine is a good initial guess. The problem of the sum rate maximization is reduced only to the description of the interference. Therefore the number of variables can be reduced by a factor of two third for the matching network, as the interference function

REFERENCE

only requires the input impedance of the matching network. This reduced problem has size of $N_{\text{var}} = 2 \cdot N_{\text{Rel}} + 2 \cdot N_{\text{R}} \cdot N_{\text{Rx}} = 2 \cdot 4 \cdot 5 + 2 \cdot 4 \cdot 2 = 56$, for the same settings as above. The factor 2 from the matching network variables comes from the fact, that with pure imaginary elements in the matching network, any complex value of the input impedance can be achieved.

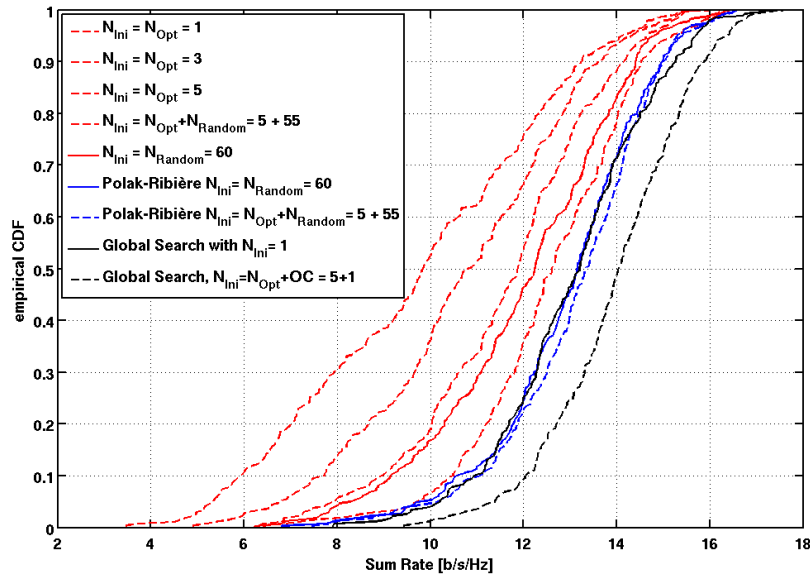


Figure 4.10: Comparison of the number of initial values used.

Figure 4.10 shows the performance of the steepest ascent algorithm, with the pre-optimized initial values (three red dotted curves on the left). We see, that using the five best pre-optimizations leads to a performance almost as good as initializing the algorithm with 60 random vectors (red solid curve). To push the optimization even further, we can combine these two techniques and take the best optimization from the five best pre-optimized initial values and 55 random initial values (red dotted curve on the right). This leads to a 0.5 [b/s/Hz] improvement at the mean and a 1.5 [b/s/Hz] improvement for the lowest 10% of the rates, than only considering random values.

Applying this to the method of Polak-Ribière (blue dotted curve), however, does not improve the results as much as with the steepest ascent method. A sum rate of only about 0.1 [b/s/Hz] higher is achieved by using pre-optimized initial values in combination with the method of Polak-Ribière.

Finally, this method is applied to the heuristic GlobalSearch routine. As mentioned in Section 4.3.2, GlobalSearch is less dependent on the initial value and therefore, the initial value is chose to be open circuited for the relays. With five optimized

initial values plus the standard open circuit initial value, an improvement of almost 1.0 [b/s/Hz] can be achieved (black dotted curve) compared to initializing only by the open circuited value (black solid curve).

4.4.2 Post Refinement of GlobalSearch by Gradient Search

When the problem of gradient search is, that it may run into non optimal local maximas, the questions remaining for the heuristic solvers are: "How good are the results after all?" and "Can they be improved any further?"

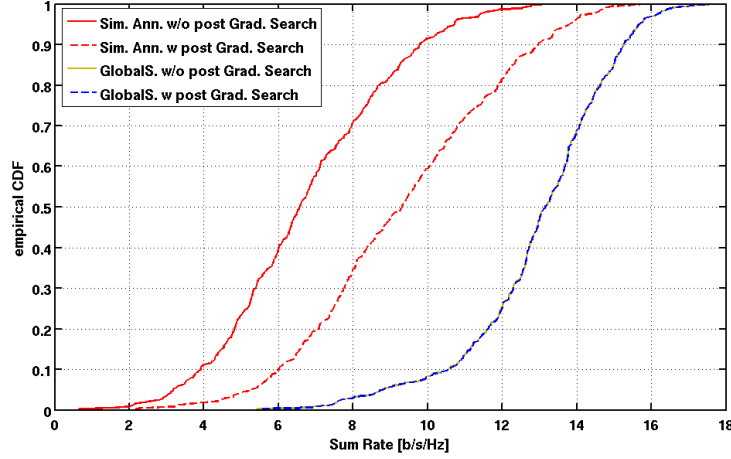


Figure 4.11: Comparison the heuristic solvers with and without a post refinement by gradient search.

The approach in finding the answers, is to use the gradient search routine on top of the heuristic solvers as a refinement. Figure 4.11 shows the performance of the Simulated Annealing and the GlobalSearch algorithm (solid red and solid yellow curves). The dashed lines show the result, when gradient search was added on top of the heuristic solvers (red for Simulated Annealing and blue for GlobalSearch). This shows, that the poor results of the Simulated Annealing algorithm does not lead to any good initial value for the gradient search as after the refinement the performance is still about 5 [b/s/Hz] worse, than the performance of GlobalSearch. Second, it shows that the performance of GlobalSearch is quite good, as any post refinement of gradient search does not lead to any significant improvement.

4.4.3 Stepwise Relay Improvements

In the previous Sections, we saw the performance of different methods for three relays per user. The number of relays was kept small for the analysis of the algorithms, so that complexity effects diminishing the performance were avoided. Increasing the number of relays might result in worse sum rates. Therefore we will have a look at the performance of the optimization and how it can be pushed in the following. For the results shown below, the number of relays were increased to seven, if not mentioned specifically.

In Figure 4.12 we see the performance of the GlobalSearch algorithm, optimizing a 2×2 MIMO system, with seven relays and one receiving antenna per user (red curve). The black curve shows the performance of the algorithm optimizing only three relays per user (c.f. red curve in Figure 4.9). Actually this should be a lower

limit of the red curve, as one solution for seven relays is to optimize only three of them and open circuit the remaining four. However this is only the case for about 85% of the cases, the lowest 15% actually lead to a worse solution than only optimizing three relays. This shows, that the GlobalSearch optimization might not perform very good on larger problems, i.e. reducing the size of the problem results in a better sum rate.

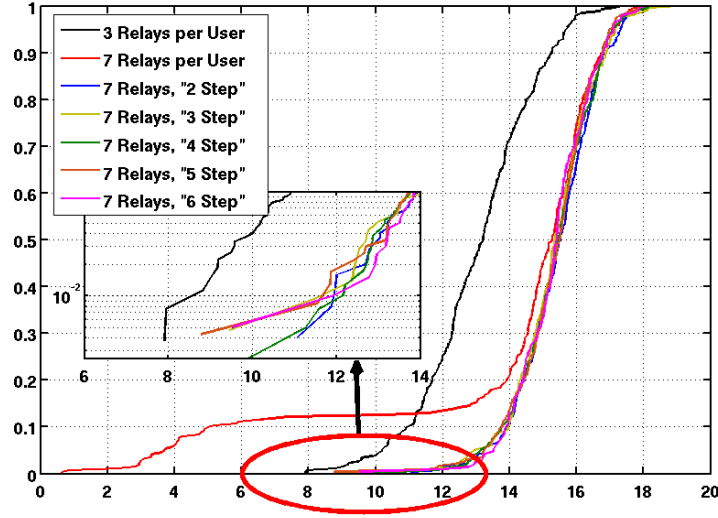


Figure 4.12: Comparison of the number of initial values used.

Therefore one approach to prevent GlobalSearch of running into a low rate, is to reduce the number of relays to optimize and increase them stepwise. The blue curve shows the result of the optimization, when GlobalSearch is allowed to optimize only two relays. Once finished, two additional relays are considered so that in total four relays per user are optimized. This is repeated until the total number of relays is reached (in this case four times, $N_{\text{Rep}} = \lceil \frac{N_{\text{Relays}}}{N_{\text{Step}}} \rceil = \lceil \frac{7}{2} \rceil = 4$). This leads to a tradeoff between the precision of the routine and the run-time, as a smaller number of relay steps (N_{Step}) will lead (most probably) to a better result, but also to a larger number of repetitions and therefore it will take a lot longer ($\approx N_{\text{Rep}} * T_0$, for T_0 , the time for one optimization).

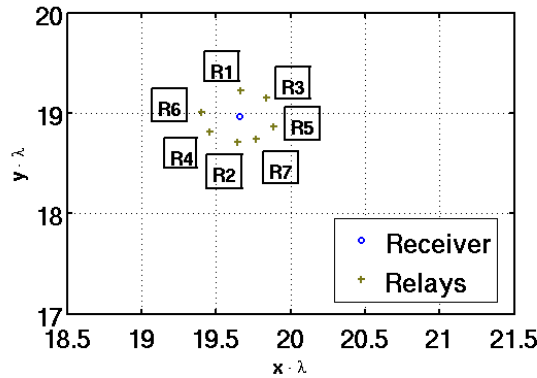


Figure 4.13: Example of choosing the relays for stepwise optimization.

The first relay is thereby chosen at random. For the following relays, the algorithm takes always the next free relay across the receiver. Figure 4.13 shows an example on how the relays would be chosen for this setting.

Back in Figure 4.12, the yellow curve shows the optimization for a stepwise increment of $N_{\text{Step}} = 3$. Therefore $N_{\text{Rep}} = 3$ had to be taken. As for $N_{\text{Step}} = 4$, $N_{\text{Step}} = 5$ and $N_{\text{Step}} = 6$ (with each $N_{\text{Rep}} = 2$), it leads almost to the same result. It can also be seen, that none of the stepwise optimized solvers has a significant low rate outlier (logarithmic scaled subplot), therefore we can say, that the outliers from the direct optimization can be avoided, when a single repetition is added.

Chapter 5

Results

In the following, the results of the thesis will be discussed. The performance of the optimization routine will be shown for different settings, i.e. for different number of relays, receiving antennas per user, users, relay placings, ... If not any further mentioned, the same settings will be used, as in Section 4, i.e. we will look at a 2x2 MIMO system with one receive antenna per user and three relays, as shown in Figure 2.2. The relays in this system will be lossless, i.e. the impedances will be pure imaginary.

5.1 Introduction of Measures for Comparison

To be able to rate the results, on how good they are, the performance will be compared to TDMA. Additionally theoretical performance limits will be shown, in order to see by how much the performance could be pushed at maximum.

5.1.1 Uncoupled Relay Rates

One of the logical performances to compare the use of loaded antennas to, is the same setting without any coupling among the relays. Logically, the "uncoupled relays rate" should be smaller than including and adapting the coupling to our needs. If no higher rate can be achieved, the whole idea of using passive relays would fail.

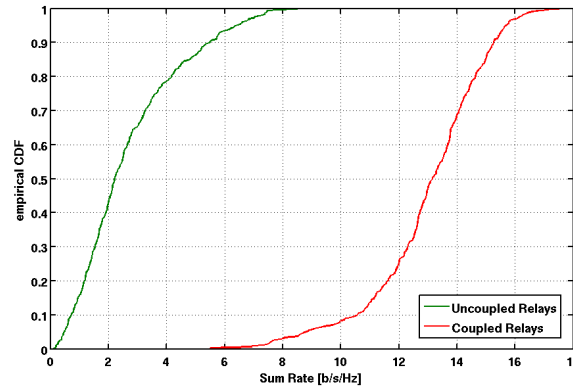


Figure 5.1: Comparison of uncoupled relays and optimized coupled relays.

In Figure 5.1, the green solid line shows the performance if no coupling among the relays and receivers exist. It is clear, that the rates including relay coupling (red solid line) are much larger than without any coupling.

5.1.2 TDMA Rates

The next performance, the optimized rates are compared to are the TDMA rates for the equivalent setup. Therefore, the relays are again assumed to be uncoupled from the receivers and the transmit/receive pairs are assumed to divide the time equally among each other for transmission.

FORMULAS (PRELOG-FACTOR)

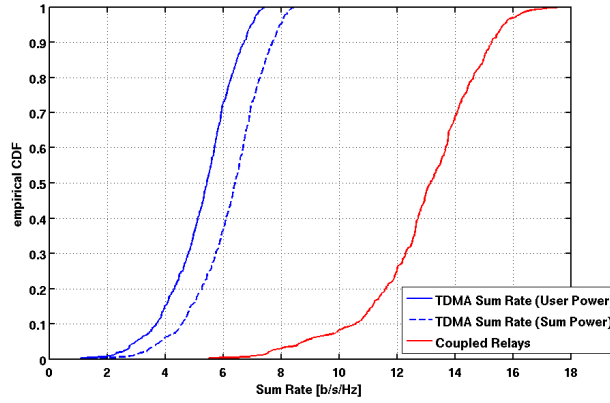


Figure 5.2: Comparison of the TDMA rate and optimized coupled relays.

In Figure 5.2, the blue solid line shows the performance if TDMA was applied under the user-power constraint (i.e. the limit of the transmit power is given per user and therefore the same for each user as in the coupled relay case) and the relays were uncoupled from the receivers. The blue dashed line shows the performance of TDMA under the sum power constraint (i.e. the limit of the transmit power is given by the total transmit power and therefore the power per user in TDMA is N_{User} times the power per user in the coupled relay case - here two times). As before, the rates including relay coupling (red solid line) are much larger than without any coupling and TDMA. Of course this comparison is more dependent on the choice of the settings (especially the choice of the number of transmit-receive pairs) and we will see different behaviors in the following sections.

5.1.3 Signal-Interference-Ration (SIR) Rates

As we are addressing the problem of interference, a good measure is the SIR-rate. It is calculated similar to the SINR-rate(?), however it only considers the interference and not the noise. As we said, in high SNR regime, the interference is the main diminishing factor for the rates (c.f. Section 2.4), the SIR-rates will give us an indicator, on how good we optimized the relays. Example curves of the SIR-rates (blue dashed lines) can be seen in Figures 5.5 to 5.7.

5.1.4 Relays as Fully Cooperation Receivers - Limit

The remaining two function to which the optimization algorithms are compared against will give limits on how good the method of loaded antennas can be at best. The first approach is to see the relays as fully cooperation receivers. Therefore

the number of observations the receiver has on the incoming signals is increased to $N_{\text{Rx}} + N_{\text{Relays}}$. As we choose the number of relays always strictly larger than the number of interferer, this method will always lead to zero interference.

The performance of the fully cooperation relays can be seen in Figure 5.3 (black solid curve). At median it is almost 2 [b/s/Hz] higher, than the optimized rate of the passive coupled relays. For the best 10% of the cases this is reduced to 1 [b/s/Hz] and less, for the worst 10% of the cases this lies in between 2.5 [b/s/Hz] and 4.7 [b/s/Hz].

5.1.5 Multiport Matching - Limit

The Multiport Matching Rate can be found here [1]. It has been shown that this is the optimal setting for a matching network (without considering any coupling among the receivers, and any relays). For the comparison with the coupled relays, the relays are, as in the previous section, assumed to be fully cooperating receiver antennas. Therefore the number of observations one receiver has, is again $N_{\text{Rx}} + N_{\text{Relays}}$. And it can be expected, that it is higher than the optimized coupled relays rate.

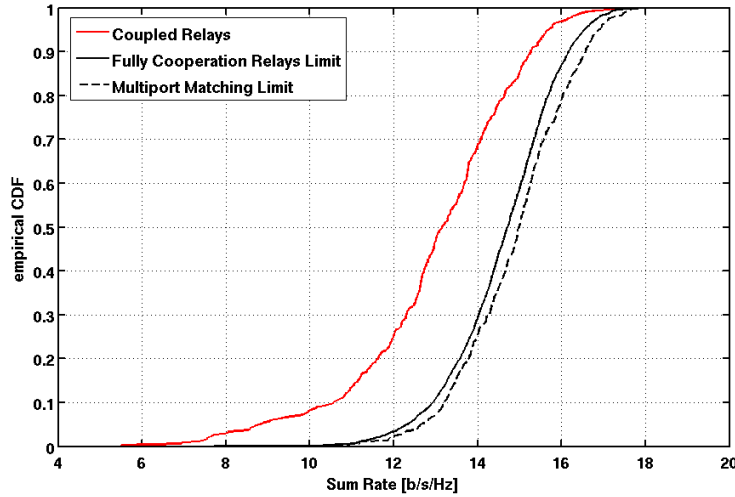


Figure 5.3: Comparison of the full cooperation relay rates, the multiport matching rate and optimized coupled relays rate.

In Figure 5.3 this limit is shown by the black dashed line. It is a little bit higher than the fully cooperation relays performance.

5.2 Relay Placing

Before analyzing the solver with different settings, the placing of the relays around a receiver is discussed a bit more in detail. Figure 5.4 shows, by which criteria, the relays were placed. The red solid line denotes a zone around the receiver, in which no relays must be placed. The red dashed line shows the maximum distance at which the relays may be placed away from the receiver. Within those two lines, the relays are thrown uniformly distributed. The blue line around the relay at the right bottom denotes a zone in which no other relay may be placed, i.e. the minimum distance between each relay. If there is a violation by the relay distances, all the relays are thrown again.

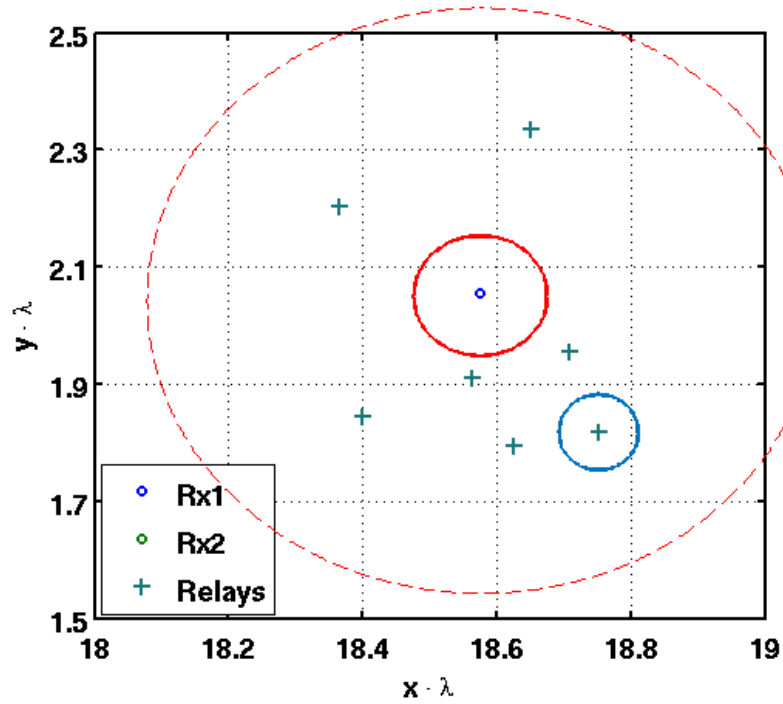


Figure 5.4: Placing the relays around a receiver uniformly distributed on a disk.

The minimum receiver distance and the minimum relay distance might differ, however, if not specially mentioned, they are assumed to be both 0.1λ .

5.3 Relays to Zeroforce Interference

5.3.1 One Interferer

5.3.2 Two Interferer

5.3.3 Three Interferer

5.4 Relay versus Rx Antenna Zeroforcing

5.5 Low SNR performance

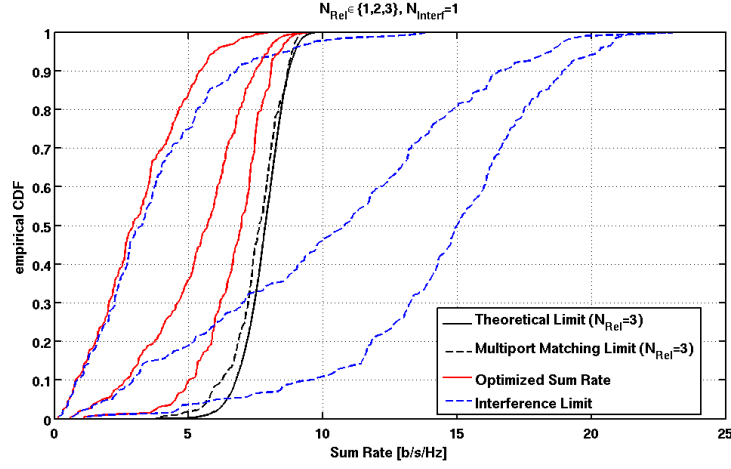


Figure 5.5: Sum rates for one interferer and one receiver with $N_{\text{Rel}} \in \{1, 2, 3\}$.

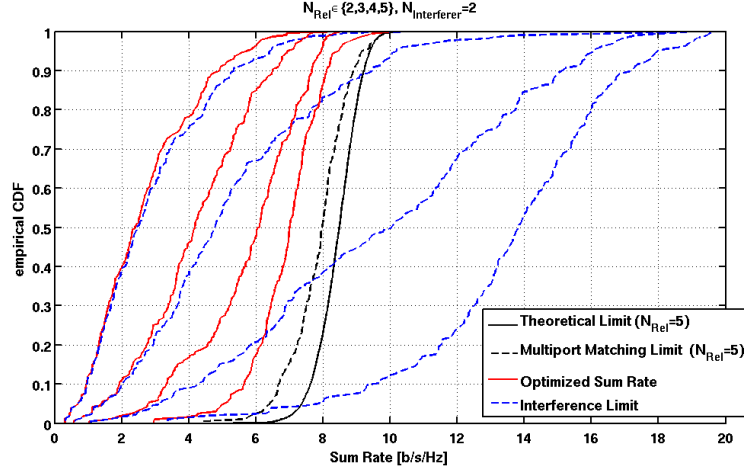


Figure 5.6: Sum rates for two interferer and one receiver with $N_{\text{Rel}} \in \{2, 3, 4, 5\}$.

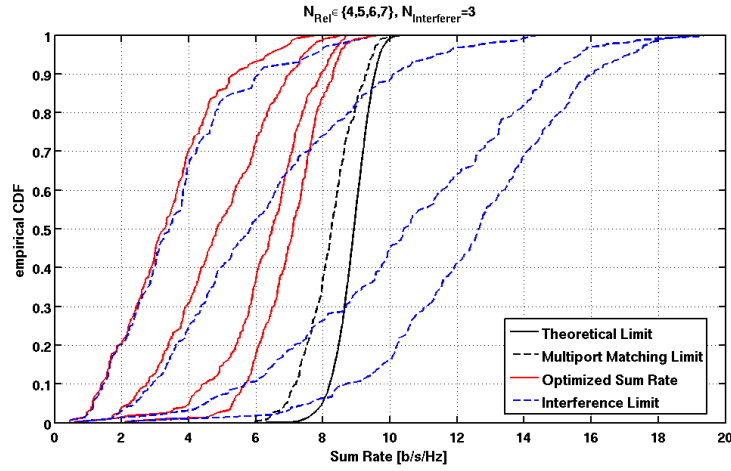


Figure 5.7: Sum rates for three interferer and one receiver with $N_{\text{Rel}} \in \{4, 5, 6, 7\}$.

Chapter 6

Conclusion and Outlook

6.1 Conclusion

6.2 Future Work

Bibliography

- [1] M. Ivrlac and J. Nassek, “Towards a circuit theory of communication,” in *IEEE Transactions on Circuits and Systems, CAS*, July 2010.
- [2] Antenna Magus, “ANTENNA MAGUS - Utilities information — The leading Antenna Design Software tool. — Antenna Design. Simplified,” 2015. [Online; accessed 16-May-2015].
- [3] Y. Hassan and A. Wittneben, “Rate maximization in coupled mimo systems: A generic algorithm for designing single-port matching networks,” in *IEEE International Symposium on Personal, Indoor and Mobile Radio Communications, WCNC*, Sept. 2013.
- [4] R. Q. Twiss, “Nyquist’s and Thevenin’s Theorems Generalized for Nonreciprocal Linear Networks,” *Journal of Applied Physics*, vol. 26, pp. 599–602, May 1955.
- [5] C. P. Domizioli and B. L. Hughes, “Front-End Design for Compact MIMO Receivers: A Communication Theory Perspective,” *IEEE Transactions on Communications*, vol. 30, pp. 2938 – 2949, Oct. 2012.
- [6] K. B. Petersen and M. S. Pedersen, “The Matrix Cookbook,” Nov. 2012. Version 20121115.
- [7] Wikipedia, “Lp space — Wikipedia, the free encyclopedia,” 2015. [Online; accessed 06-May-2015].
- [8] Wikipedia, “Conjugate gradient method — Wikipedia, the free encyclopedia,” 2015. [Online; accessed 11-May-2015].
- [9] R. Fletcher and C. M. Reeves, “Function minimization by conjugate gradients,” *The Computer Journal*, vol. 7, no. 2, pp. 149–154, 1964.
- [10] E. Polak and G. Ribiere, “Note sur la convergence de méthodes de directions conjuguées,” *ESAIM: Mathematical Modelling and Numerical Analysis - Modélisation Mathématique et Analyse Numérique*, vol. 3, no. R1, pp. 35–43, 1969.
- [11] S. Kirkpatrick, C. D. Gelatt, and M. P. Vecchi, “Optimization by simulated annealing,” *SCIENCE*, vol. 220, no. 4598, pp. 671–680, 1983.
- [12] The MathWorks, Inc., “How Simulated Annealing Works - MATLAB & Simulink - MathWorks Schweiz,” 2015. [Online; accessed 11-May-2015].
- [13] The MathWorks, Inc., “How GlobalSearch and MultiStart Work - MATLAB & Simulink - MathWorks Schweiz,” 2015. [Online; accessed 11-May-2015].